State University of New York Report

Large Eddy Simulations and Direct Numerical Simulations of High Speed Turbulent Reacting Flows

by

P. Givi, C.K. Madnia, C.J. Steinberger and A. Tsai
Department of Mechanical and Aerospace Engineering
State University of New York
Buffalo, NY 14260

Semi-Annual Report Submitted to
NASA Langley Research Center

Summary of Activities Supported Under Grant NAG 1-1122

for the Period

November 1, 1990 - May 1, 1991

TABLE OF CONTENTS

Abstract

This research is involved with the implementations of advanced computational schemes based on large eddy simulations (LES) and direct numerical simulations (DNS) to study the phenomenon of mixing and its coupling with chemical reactions in compressible turbulent flows. In the efforts related to LES, we have initiated a research program to extend the present capabilities of this methods for the treatment of chemically reacting flows, whereas in the DNS efforts, we have focused on detail investigations of the effects of compressibility, heat release and non-equilibrium kinetics modeling in high speed reacting flows. Our efforts to date, have been primarily focused on the simulations of simple flows, namely homogeneous compressible flows and temporally developing high speed mixing layers.

This report provides a summary of our accomplishments during the second six months of the research supported under Grant NAG 1-1122 sponsored by NASA Langley Research Center administrated by Dr. J. Phil Drummond of the Theoretical Flow Physics Branch.

1. Summary of Accomplishments to Date

During the second half of the first year of activities under this research, we have been primarily involved with the continuations of our tasks in the same two directions as that indicated in our first report. Namely: (1) development of subgrid closures for LES of compressible reacting flows, and (2) Understanding the mechanisms of mixing and reaction in high speed combustion. In the efforts related to the first task, our efforts are concentrated on the simulations of homogeneous reacting turbulence, whereas in the second task direct numerical simulations of a high speed reacting mixing layer is the subject of main focus. Below, a summary of our efforts during the second 6 months of this research is provided and detail descriptions are furnished in Appendix I and Appendix II.

1.1. Large Eddy Simulations of Compressible Reacting Flows:

Our major goal in this effort is to initiate a program to extend the present capabilities of LES for the treatment of chemically reacting flows. In the efforts to date, we have been primarily concerned with *a priori* analysis of subgrid fluctuation in a compressible homogeneous flows. This analysis is mainly involved with constructing the shapes of the simulated PDF's within the subgrid. This work is currently in progress, and Appendix I and Appendix II provides a write-up on some of our recent progress. Our conclusions, some of which are indicated in these appendices, are summarized below:

The primary objective of the research conducted to date has been to develop and evaluate mathematical models based on the PDF methods for predicting the phenomena of mixing and chemical reaction in turbulent reacting flows. The research was initiated in two parallel but related directions:

1. Development of improved turbulence closures based on PDF methods for the purpose of predicting the statistical behavior of reacting turbulent flows, and also for statistical treatment of the behavior at the subgrid.

2. Implementation of Direct Numerical Simulations (DNS) to provide data for evaluation of the performance of the closures for both Reynolds averaging and subgrid closures.

Based on our efforts thus far, we have been able to draw the following conclusions:

1. In the context of single-point PDF formulation, the mapping closure of Kraichnan (1989)

provides the most satisfactory results.

2. The main deficiency of the above mentioned mapping closure (or any other single-point PDF model) is associated with its incapability in predicting the frequency (or length) scale of PDF evolution.

3. The EDQNM spectral closure provides a reasonable means of overcoming the deficiency mentioned above in transport of conserved scalar quantities.

4. The extension of the mapping closure for PDF formulation at two-point is very difficult. Among the other currently available alternatives, the LMSE closure is the simplest to use but does have drawbacks.

5. Preliminary results obtained by means of two-point PDF formulation based on the LMSE model and the EDQNM closure indicate that the evolution of the relevant length scales is somewhat insensitive to the rate of chemical reaction in a chemistry of the type $A + B \rightarrow$ *Products*. Therefore, the EDQNM of a conserved scalar can be used in conjunction with the mapping closure at single-point for both non-reacting and reacting scalars.

6. With the utilization of the mapping closure, the rate of fuel consumption in plug flow reactors can be predicted by a closed form algebraic relation. The results obtained by this relation compares very well with DNS data for a stoichiometric mixture under equilibrium condition. In fact, to the best of our knowledge, this relation is more satisfactory than any other suggested correlations (empirical or theoretical) available in the literature within the past thirty years!

7. The extension of the model to account for non-stoichiometric mixtures has been done. It is shown that for such mixtures, the consumption rate of fuel can not predicted by a simple algebraic relation; rather, it can only be expressed in terms of complex integrals.

In addition to the primary conclusions listed above, we have also been able to show that:

8. The β-density does reasonably well in approximating the single point PDF distribution of a conserved scalar property, if the evolution of its variance is known ***a priori***.

9. With the implementation of the β-density, it is also possible to develop a closed form algebraic solution for the rate of reactant conversion under the assumptions indicated in

item (6).

10. The solution corresponding to that in item (9) for non-stoichiometric mixtures would also be in the form of complex integrals.

11. Despite its simplicity, the β-density is only applicable for description of "simple" distributions. It is not applicable for bimodal distributions, and it can not predict the subsequent evolution of the PDF, if the distribution is not of β-type initially. Furthermore, it can not be extended for predictions of non-equilibrium reactions and there are no firm mathematical proofs to justify its use.

1.2. Direct Numerical Simulations of High Speed Reacting Mixing Layers:

This work is involved with the assessment of the roles of compressibility and heat release, and the non-equilibrium effects of chemical kinetics on the compositional structure of the flame in high speed reacting mixing layers. This work has been mainly motivated due to the interest of NASA in understanding the global and detail mechanisms of mixing and chemical reactions in high speed flows.

Our current efforts in this work are directed toward understanding one important phenomenon. Namely, the exact influences of the Damköhler number on the statistical compositional structure in a compressible mixing layer under the influence of non-equilibrium exothermic chemical reactions. It must be indicated that our previous work on examining the role of Damköhler number in incompressible flows showed that the effects of this parameter is rather insensitive to the procedure by which it is varied. Our current efforts, however, indicates that this is not the case in compressible reacting layers. We do not have a write-up of our results addressing this issue. Nevertheless, Appendix III provides a summary of some of our related work in this area.

2. Published Work

The following publications and reports have resulted from our efforts during the second six months of this research:

2.1. Conference Papers:

C. J. Steinberger, "Model Free Simulations of a High Speed Reacting Mixing Layer," Presented at the AIAA Northeastern Regional Student Conference, held at Worcester Polytechnic Institute, Worcester, MA. April 15, 1991.

2.2. Honors:

Mr. Craig Steinberger was the winner of the first award in *Graduate Full Paper Competition* at the AIAA Northeastern Regional Student Conference, held at Worcester Polytechnic Institute in Worcester, MA (April 1991). He has been invited to participate at the National AIAA Student Conference to be held at Reno, Nevada during the AIAA Aerospace Sciences Meeting in January 1992.

Appendix I

This Appendix is provided by Dr. Cyrus K. Madnia, a Post-Doctoral Research Associate working on this project.

SUMMARY

Direct Numerical Simulations (DNS) are performed to investigate the phenomena of mixing in a decaying two-dimensional, homogeneous turbulent flow under non-reacting and reacting unpremixed conditions. In the reacting case, a second order stoichiometric irreversible reaction of the type $A + B \rightarrow Products$ is considered. An infinitely fast chemical reaction rate is assumed without including the effects of non-equilibrium chemistry. The data obtained by DNS is utilized to examine the behavior of the scalar field in a stochastic manner. This involves the extraction of Probability Density Functions (PDF's) of the scalar field from the DNS results. The examination of the data in this manner provides a useful mechanism for assessing the range of validity of PDF methods for turbulence modeling in Reynolds averaged equations, and for subgrid closures in Large Eddy Simulations (LES).

Simulations are performed of flows with various levels of compressibility to examine its effects on the structure of the flow field. In the low compressibility regime, the flow exhibits features similar to those observed in previous incompressible simulations, whereas in the high compressibility case, shocklets are formed. In both cases, the simulated results indicate that the PDF of a conserved Shvab-Zeldovich scalar quantity, characterizing the mixing process, evolves from an initial double-delta distribution to an asymptotic shape that can be approximated by a Gaussian distribution. During this evolution, the PDF can be approximately described by a Beta density and also exhibits features compatible with those predicted by the mapping closure of Kraichnan. The main difference exhibited between the two cases is the time scale of decay of the rms of the scalar by which the PDF is characterized. A discussion of the results is provided with a focus on their relevance towards turbulence modeling and LES closure. A brief review is also provided of recent related contributions in PDF modeling and LES in order to provide a framework for anticipated continuation of the present work.

1. INTRODUCTION

In review of recent computational work on turbulent reacting flows, Drummond (1991), Oran and Boris (1987) and Givi (1989) indicate the need for further development in both the methodology and the implementation of Direct Numerical Simulations (DNS) and Large Eddy Simulations (LES). According to these reviews, the results of previous and ongoing works towards the development of advanced numerical algorithms for simulating reacting turbulent fields have been successful, thus warranting their continued utilization for future implementations. With the broad knowledge gained to date, it is now widely accepted that foreseeable developments in advanced computational facilities will not be sufficient to relax the restriction of DNS to flows having small to moderate variations of the characteristic length and time scales (Rogallo and Moin, 1981; Reynolds, 1990; Schumann and Friedrich, 1986, 1987, Givi, 1989). Nevertheless, DNS can be (and have been extensively) used to enhance our understanding of the physics of chemically reacting turbulent flows by providing specific information concerning the detailed structure of the flow, and by furnishing a quantitative basis for evaluating the performance of turbulence closures. In this sense, DNS have provided an effective tool for such studies and have established useful guidelines for future investigations.

LES appear to provide a good alternative to DNS for computing flows having ranges of parameters similar to those encountered in practical systems (Reynolds, 1990; Hussaini *et al.*, 1990, Ferziger, 1981, 1983, Schumann and Friedrich, 1987). This approach has a particular advantage over analogous Reynolds-averaging procedures in that only the effects of small-scale turbulence have to be modelled. However, despite their success for the analysis of both incompressible (Ferziger, 1981) and compressible (Erlebacher *et al.*, 1987) flows, they have seldom been employed for calculations of reacting turbulence. This is primarily due to appearance of enormous unclosed terms in the transport equation governing the evolution of the filtered quantities in LES. In these equations, the correlations amongst the scalar variables must be accurately modelled in order to provide a realistic estimate of the reactant's conversion rates.

A methodology which has proven useful for predictions of turbulent reacting flows is based on the Probability Density Function (PDF) or the joint PDF of the scalar variables which characterize the field (O'Brien, 1980; Pope, 1979, 1985, 1990a). A particular advantage of the method is the fundamental property of the probability density, namely that it provides

the complete statistical information about the behavior of the variable. This, in comparison with moment methods, provides a unique advantage in that once the distribution of the PDF is known, the mean and higher order moments of the reaction rate (or any other functions of the scalar field) can be directly determined without a need for further closure assumptions. The implementation of PDF methods in conjunction with the Reynolds- and/or Favré-averaged form of the equations of turbulent combustion has proven very successful (For an excellent recent review see Pope (1990a)). During the past 15 years, these methods have been used for simulating a variety of reacting flow configurations and, in many cases, the predicted results have been indicative of the higher accuracy of these methods in comparison with conventional moment methods. Based on this indication, it is safe to state that presently, from the statistical point of view, PDF methods are the most attractive choice for the description of chemically reacting turbulent flows.

A similar scenario may be surmised to be the case when the PDF methods are used in the context of subgrid closures for LES. In this case, the PDF (or the joint PDF) of the scalar variables within the ensemble of grids (identifying the large scales of the flow) may uniquely determine the subgrid average value of the reaction rate (or other functions of the scalar variables). This PDF, in conjunction with an appropriate model for the hydrodynamic fluctuations within the subgrid, may facilitate the implementation of LES for the analysis of reacting turbulence.

Our main goal in this work is to initiate an assessment of the use of PDF methods for their possible future implementation in LES, as well as to further our investigation of the PDF methods in modeling turbulent combustion problems. The approach followed is similar to those previously used in the *a priori* analyses. Namely, the data obtained by DNS are utilized to construct the appropriate PDF's that can be used for either turbulence modeling or subgrid closures. We are currently in a preliminary stage of our work, especially in tasks directed at subgrid modeling.

In order to establish a framework for the discussion of the results, a review is provided of PDF methods and subgrid closures in Section 2. This review is rather brief and is presented solely for the purpose of providing a reference for the remainder of the chapter. However, the reader is referred to other collective works and survey articles which discuss these statistical methods in greater detail. Also, the discussion on PDF methods focuses on the treatment of scalar quantities alone, without including the treatment of scalar-velocity

PDF's. The specification of the problem under current scrutiny is provided in Section 3, in which the relevance of some of the characteristic variables are expressed, together with a description of the geometrical configuration and the initialization procedure. The results of simulations are presented in Section 4, in which we place an emphasis on the use of stochastic methods for modeling of the mixing phenomenon. This chapter ends in Section 5, where we summarize our findings, and also provide some speculations and suggestions for future work, some of which are currently under way.

2. BACKGROUND REVIEW

2.1. PDF METHODS:

In the majority of previous work on the computational treatment of turbulent combustion, statistical methods have generally been employed. These methods involve the representation of physical variables in a stochastic sense, and in conjunction with appropriate transport equations, predict the approximate behavior of the flow field. In the framework of such methods, the physical quantities are treated as *random* variables, and the transport equations describing the evolution of these quantities are used in such a way as to yield their stochastic variations. At present, two general types of strategies are identified which can be utilized for statistical treatment of turbulent combustion problems (Libby and Williams, 1980): (1) the moment method, and (2) the Probability Density Function (PDF) method. In the first approach, "averages" (or "means") of the relevant physical variables are introduced, and the governing transport equations are subsequently averaged. These averages are generally defined in such a way to yield the desired mathematical properties and are usually introduced in the form of time-, ensemble-, or Favré-averages. The second approach, the PDF approach, relies directly on the PDF of these variables by which the desired moments can be obtained.

Moment methods usually involve the determination of the statistical means by virtue of solving transport equations for the various unclosed moments of the equations. These equations provide, in a sense, a description of the variables at one level higher than the equations for the mean values (first moments). This results in explicit transport equations for the second order moments. These equations, however, are still not in a closed form, due to the appearance of the unclosed third order correlations which require further modeling. Regardless of the degree of truncation of the higher moments, the closure problem always remains, and transport equations at any level require modeling at higher orders.

The primary advantage of moment methods is their relative ease of use in engineering applications. Most models suggested in the literature can be implemented directly into computer codes developed for laminar flows. This allows the engineer to economically obtain approximations to combustion problems for many different sets of flow conditions. The results obtained in this way have, in many cases, exhibited good agreement with experimental measurements. This has been a major factor in justifying the use of moment methods in turbulent combustion and it appears that these methods will remain popular for engineering applications for the near future.

The closure based on the second approach, the PDF method, has proven very useful in the theoretical description of turbulent reactive flows (Hawthorne *et al.*, 1949). The philosophy of this approach is to consider the transport of the PDF's rather than the finite moments of the statistical variables. The key advantage of the method is the fundamental property of the PDF, namely that the mean reaction rate (and any other functions of the scalar) can be evaluated directly from the PDF. Representing the scalar field involving σ species by $\Phi = (\phi^1, \phi^2, \ldots, \phi^\sigma)$, and the reaction conversion rate of species α by $\omega_\alpha(\Phi)$, the mean of this rate (denoted by $< >$) can be written as:

$$< \omega_\alpha >= \int_{-\infty}^{+\infty} \mathcal{P}_1(\underline{\Xi})\omega_\alpha(\underline{\Xi})d\underline{\Xi} \tag{1}$$

In this equation, $\underline{\Xi}$ represents the scalar space and $\mathcal{P}_1(\underline{\Xi})$ is the PDF of the scalar variable at a point, defined so that:

$$\mathcal{P}_1(\underline{\Xi})d\underline{\Xi} = \text{Probability } (\underline{\Xi} \leq \Phi \leq \underline{\Xi} + d\underline{\Xi}) \tag{2}$$

where $d\underline{\Xi} = (d\xi^1, d\xi^2, \ldots, d\xi^\sigma)$ denotes an elemental hypervolume at $\underline{\Xi}$.

The scalar PDF, $\mathcal{P}_1(\underline{\Xi})$, defined in Eqs. (1)-(2), is in its simplest form in that it contains information only about the scalar variables, Φ. Also, it governs the probability distribution only at a single point. However, it contains much more information than is required to determine the mean value of any functions of the random variables Φ. Therefore, its evaluation in comparison to direct evaluation of $< \omega_\alpha >$ (if it could have been done) is understandably more difficult. Nevertheless, since $\mathcal{P}_1(\underline{\Xi})$ includes all the statistical

information about the scalars, its determination is in many ways more useful than that of the mean values.

A systematic way of evaluating a PDF is to obtain and solve a transport equation governing its evolution. A transport equation for $\mathcal{P}_1(\underline{\Xi},\ \underline{\Xi} = \xi^1, \xi^2, \ldots, \xi^\sigma)$ can be constructed by relating the PDF to $\Phi(\underline{x}, t)$ in terms of Dirac-delta functions (Pope, 1979, 1985, 1990a; O'Brien, 1980, 1981, 1986):

$$\mathcal{P}_1(\underline{\Xi}) =< \varrho(\underline{x}, t) > \tag{3}$$

where ϱ is the single-point fine grained density defined by:

$$\varrho = \prod_{\alpha=1}^{\alpha=\sigma} \delta(\xi^\alpha - \phi^\alpha) \tag{4}$$

From the appropriate conservation equations for the scalar field and Eqs. (1)-(4) one can obtain transport equation describing the evolution of the PDF. Limiting the formulation to that of a constant density Fickian diffusion flow, we have (see O'Brien, 1980 for a complete derivation):

$$\frac{\partial \mathcal{P}_1}{\partial t} + < \underline{V} \cdot \nabla \varrho >= -\frac{\partial}{\partial \xi^\alpha}(\omega_\alpha \mathcal{P}_1) + \Gamma < \nabla^2_{\underline{x}} \phi^\alpha \frac{\partial \varrho}{\partial \xi^\alpha} > \tag{5}$$

Here, $\underline{V}$ is the velocity field and Γ is the diffusion coefficient of the species. From this equation, it can be seen that the effects of reactivity and diffusivity (the terms on the RHS) are to transport the PDF into the composition space ($\underline{\Xi}$), whereas the convective transport is a physical space phenomenon. Furthermore, it is shown that the influences of $\omega_\alpha(\Phi)$ in the composition space appear in closed form. However, models are needed for the closures of the molecular mixing term (second term on the RHS) and the turbulent convection term (second term on LHS).

Since the term that includes the interaction between the scalar variables through the reaction rate ω_α appears in a closed form in Eq. (5), in what follows we limit the discussion to the transport of a single reacting scalar (i.e. $\sigma = 1$) which is being convected by the

velocity field. In this frame, the diffusive transport may be expressed as (O'Brien, 1980, 1981):

$$< \nabla^2_{\underline{x}} \phi \frac{\partial \varrho}{\partial \xi} >= \frac{\partial}{\partial \xi} Lim_{\underline{x}_2 \to \underline{x}_1} \nabla^2_{\underline{x}_2} [E(\xi_2|\xi_1)\mathcal{P}_1(\xi_1)] \tag{6}$$

Here, $E(\xi_2|\xi_1)$ represents the expected value of the scalar at $\underline{x}_2$ from its known value at $\underline{x}_1$. This equation explicitly reveals a fundamental difficulty associated with the PDF formulations, namely that the transport equation for a one-point PDF ($\mathcal{P}_1(\xi, \underline{x}, t)$) requires information about the second point, $\underline{x}_2$. In general, n-point PDF's, $\mathcal{P}_n(\xi_1, \xi_2, \ldots, \xi_n, \underline{x}_1, \underline{x}_2, \ldots, \underline{x}_n, t)$ require information about the $n+1$th point, $\underline{x}_{n+1}$. This is further demonstrated by considering the transport of $\mathcal{P}_n$ in the compositional space (Ievlev, 1970, 1973; Kuo and O'Brien, 1981):

$$\frac{\partial \mathcal{P}_n}{\partial t} + \sum_{q=1}^{n} \frac{\partial}{\partial \xi_{(q)}} [\omega(\xi_{(q)})\mathcal{P}_n] = \sum_{q=1}^{n} \frac{\partial}{\partial \xi_{(q)}} (C^{(q)}\mathcal{P}_n) \tag{7}$$

where:

$$C^{(q)} = \Gamma Lim_{\underline{x}_{n+1} \to \underline{x}_{(q)}} \nabla^2_{\underline{x}_{n+1}} [E(\xi_{n+1}|\xi_1, \xi_2, \ldots, \xi_n, \underline{x}_1, \underline{x}_2, \ldots, \underline{x}_n)] \tag{8}$$

and $E(\xi_{n+1}|\xi_1, \xi_2, \ldots, \xi_n, \underline{x}_1, \underline{x}_2, \ldots, \underline{x}_n)$ is the expected value of ξ_{n+1} at the point $\underline{x}_{n+1}$ based on all the values of $\xi_1, \xi_2, \ldots, \xi_n$ at $\underline{x}_1, \underline{x}_2, \ldots, \underline{x}_n$. The dependence of $C^{(q)}$ on the $n+1$th point in the transport equation for $\mathcal{P}_n$ indicates the need for a closure model which relates $\mathcal{P}_{n+1}$ to $\mathcal{P}_n$.

Despite the attractiveness of the PDF methods in obtaining a closed representation of the reaction term, there is another difficulty with the implementation of the method. This difficulty is caused by the increase of the dimensionality of the PDF as the number of scalars and/or the number of statistical points increase. This imposes a severe limit on the maximum number n in the equation for $\mathcal{P}_n$. The majority of previous work on PDF's have closed the equations at the first level ($n = 1$), and only recently has closure at the $n = 2$ level been attempted. Both these closures are reviewed in detail by Givi (1989).

2.2. LES AND SUBGRID CLOSURES:

Despite the present capability of modern supercomputers in allowing calculations with more than one million grid points, the range of length and time scales that can be resolved by DNS is substantially smaller than those of turbulent flows of practical interest. In DNS the largest computable scales are limited by the size of the computational domain and the "turn-over" time of the large scale structures; the smallest resolvable features are limited by the molecular length and the time scales of the viscous dissipation and chemical reactions. DNS therefore, in comparison to turbulence modeling, find its greatest application in basic research problems in which the scales of the excited modes remain within this band of computationally resolved grid sizes. This implies that for an accurate simulation, the magnitudes of the viscosity and the diffusivity must be large enough to damp out the unresolved scales, and the size of the computational time step must be kept small enough to capture the correct temporal evolution of the turbulent flame. In this context, since the instantaneous behavior of the flow variables is directly simulated at all spatial points at every instant, the computed data can actually be used to provide a quantitative basis for evaluating the validity of turbulence models and for assessing the performance of subgrid closures in LES.

The limitations associated with DNS may be alleviated, to an extent, by pre-filtering the transport equations (Aldama, 1990), a practice implemented in LES. This is effectively equivalent to eliminating the scales smaller than those resolvable within a given mesh. In this way, the variables can be represented on the number of grid points that are available for the simulations. This filtering procedure facilitates the simulations of flows with larger parameter ranges on a coarser grid. The disadvantage is that some modeling is required for the closure of the scales excluded by filtering. The selection between DNS and LES (and turbulence modeling for that matter) is dependent on the type of flow being considered, on the range of physical parameters that characterize the turbulent field, and the degree of desired accuracy.

A straightforward implementation of LES involves the decomposition of the transport variables into "large scale" and "subgrid scale" components. The former is related to the large scale eddies in the turbulent field, whereas the latter is the component containing the small scale fluctuations. The pre-filtering of the variable $\Phi(\underline{x}, t)$ is performed by means of the convolution integral (Ferziger, 1977, Aldama, 1990):

$$\widetilde{\Phi}(\underline{x},t) = \int\int\int_{\triangle} F\ell(\underline{x}-\underline{x}')\Phi(\underline{x}',t)d\underline{x}' \tag{9}$$

where $F\ell$ is an appropriate filter function with a characteristic length $\triangle$, and the integration is over the entire flowfield. The remaining portion of Φ from the filtered quantity is defined as the subgrid-scale field and is represented by:

$$\Phi''(\underline{x},t) = \Phi(\underline{x},t) - \widetilde{\Phi}(\underline{x},t) \tag{10}$$

The magnitude of pre-filtered averaged $\widetilde{\Phi}$ and its subgrid component Φ'', are obviously dependent on the filter type (function $F\ell$) and its size $\triangle$ (for reviews see Ferziger, 1981, 1982, 1983). The simplest choice would be a box filter with:

$$F\ell(\underline{x}-\underline{x}') = \begin{cases} 1, & \text{if } |\underline{x}-\underline{x}'| \leq \triangle; \\ 0, & \text{Otherwise.} \end{cases} \tag{11}$$

where $\triangle = (\triangle_x, \triangle_y, \triangle_z)$ represents the dimensions of the box, and the length in each direction should be larger than the original grid spacing in that direction. Other types of filters have also been suggested in the literature, each of which with computational and physical advantages as well as limitations (see Aldama, 1990 and Schumann and Friedrich, 1986, 1987).

Implementation of LES as a practical tool involves a combination of DNS for the filtered portion of the transport variable $\widetilde{\Phi}$, and modeling of the subgrid-scale portion, Φ''. The transport equations for the large scale components are obtained by filtering the instantaneous transport equations by means of implementing the filter defined by Eq. (9). In the resulting filtered equations, analogous to those in Reynolds averaged, the equations representing the large scale field contain unclosed terms involving the fluctuation of the subgrid components. The methodology practiced to date in dealing with these fluctuations is very similar to that employed in Reynolds averaging procedures. One may be able to develop and solve transport equations for the moments of fluctuations (Ferziger, 1981). These equations, analogously, contain some higher order moments which are needed to be modelled. The number of these terms are usually more than the corresponding ones that appear in Reynolds averaged transport, because some items that are zero in the Reynolds

averaging approach are non-zero when filtering is used. Correspondingly, the tasks required for modeling the subgrid fluctuations would be somewhat more complicated than those in turbulence modeling. Nevertheless, since the small scales of turbulence are believed to exhibit a more "universal" character is the main reason to anticipate that the approach based on subgrid modeling would be more promising than the procedures based on ensemble averaging closures.

Within the past two decades, there have been many attempts to fine-tune the models by optimizing the closure for subgrid fluctuations and the type of filtering to identify the large scale components of the variables. In most of these efforts, the closure of hydrodynamic fluctuations has been the subject of major concern. There has also been some results for the passive scalar simulation and modeling of velocity-scalar correlations. However, no attempts have been made for the treatment of reacting scalars and the treatment of scalar-scalar interactions. This is probably due to the consensus among the researchers in this field that until an accurate subgrid model is constructed to represent the evolution of non-reacting scalar variables, the extension to reactive flow simulations will be a difficult task.

With the new developments and progress in PDF methods and the advantages offered by such schemes over moment methods, one may anticipate that these methods may also prove useful in LES. In this case, the influences of the chemical reactions and the subgrid scalar-scalar correlations can be included by means of considering the PDF's of the fluctuating scalars within the computational grid. The advantage of using these methods for the subgrid closure is apparent since once these PDF's are known, any statistical quantity related to scalar fluctuations can be subsequently determined. This determination, although an ambitious task, is not impossible. The obvious and simplest choice is to follow an approach based on guessed PDF methods. Similar to Reynolds averaging, the first two subgrid moments of the scalar variables can be solved by LES and then the shape of the PDF can be parameterized based on these two moments. This parameterized approximate distribution can be appraised by a comparison with the "exact" shape constructed via DNS results. Similar to common practice in *a priori* assessments (Erlebacher *et al.*, 1987), the PDF distribution can be specified by performing two sets of calculations; one with a coarse mesh, the other with a fine mesh. The results obtained from the fine mesh simulations can be used to construct the PDF distribution which in turn may be used in

extensive subsequent simulations on the coarse mesh. In this setting, calculations with large transport parameters which otherwise could not be simulated on the coarse grids, are possible.

A more direct, but substantially more complicated procedure involves the solution of transport equation for the PDF's of the subgrid scalars rather than assuming their form. This approach, like its counterpart in turbulence modeling, has the advantage that the effect of scalar-scalar correlations appear in a closed form. However, models are needed for the molecular diffusion within the subgrid, and one has to resort to mixing models (a subject of current intense research) for providing the closure. The approach based on guessed PDF methods is feasible and is within the reach of present day computers. The approach based on solving the transport equation for the subgrid scale PDF might require extensive computational resources (Pope, 1990a). These models must initially be developed in a simple flow. A homogeneous flow is an excellent configuration for this purpose, and will be discussed in the next section. After the establishment of a successful model, it may be utilized for simulating more complicated flows. The extent of this utilization is dependent on the available computational resources and on the performance of the model in rigorous trials.

3. DESCRIPTION OF THE PROBLEM

The subject of our DNS is a two-dimensional homogeneous box flow under the influence of a binary chemical reaction of the type $A + B \rightarrow Products$. To impose homogeneity, periodic boundary conditions are employed in all directions of the flow, identifying the box as a homogeneous member of a turbulent universe. This periodicity allows the mapping of all the aerothermochemical variables from the physical domain into a Fourier domain, thus allowing the implementation of spectral methods for numerical simulations. The flow field is assumed to be homogeneous and isotropic, and is initialized in a similar manner to that of Passot and Pouquet (1987). This involves the superposition of a "random" velocity to a zero mean velocity and also includes random initial density, temperature, and Mach number fluctuations. These fluctuations have certain energy spectra, and the ratio between the compressible and the incompressible kinetic energy can be varied to assess the effects of compressibility. The specification of the fluctuating field with a random field is to mimic a "probabilistic" turbulent field in the context of "deterministic" DNS. This approach is similar to that followed in previous direct simulations of turbulent reacting

flows (Riley *et al.*, 1986; Givi and McMurtry, 1988; McMurtry and Givi, 1989). In a laboratory flow, these fluctuations appear as the result of interactions with the surrounding universe. Such interactions do not exist in the isolated homogeneous flow considered in our simulations. Therefore, in order to introduce the "noise," which plays a central role in laboratory turbulence, these perturbations are randomly superimposed to initialize the fluctuating field for DNS. The generated turbulence field is of decaying nature, i.e. there is no artificial forcing mechanism to feed energy to the small wave numbers. While it is more desirable to have a stationary turbulence field to focus only on the behavior of the scalar field (Eswaran and Pope, 1988; McMurtry and Givi, 1989), it is not clear how to implement such a forcing mechanism in the compressible case without modifying the behavior at low wave numbers.

The scalar fields are defined to be square waves with the two species out of phase and at stoichiometric conditions. The species field is assumed to be dynamically passive, in that turbulence influences the consequent transport of the scalar field with the neglect of reverse influences. In the non-reacting case, the trace of only one of these reactants is considered, whereas in the reacting case, the transport of an appropriate Shvab-Zeldovich variable is assumed to portray the reactant's conversion rate. This is possible by assuming an infinitely fast chemical reaction rate, and by assuming that the reactants have identical thermochemical properties. In this framework, the effects of non-equilibrium chemistry are neglected; the inclusion of such effects are postponed for future investigations.

The computational package employed in simulations is based on the modification of a code developed by Erlebacher *et al.* (1987). This code is based on a spectral collocation algorithm with Fourier trial functions. All the variables are spectrally approximated on N^2 collocation points, where N represents the number of collocation points in each of the directions. The spatially homogeneous flow evolves in time, and at each time step N^2 defines the sample data size for the purpose of statistical analysis. A third order accurate Runge-Kutta finite difference scheme is employed for temporal discretization. For a trustworthy simulation, the magnitudes of the Reynolds and Peclet numbers must be kept at moderate levels and the size of the time step should be kept small. The code is capable of simulating both two- and three- dimensional flows and we have performed both such simulations. In the presentation of our results in the next section, however, we limit our discussion to that of a two-dimensional flow.

4. PRESENTATION OF RESULTS

Computations are performed on a domain with a normalized dimension of 2π in each of the directions of the flow. With the available computational resources, a resolution of 256×256 collocation grid is attainable. With this resolution, the magnitude of the Taylor microscale Reynolds numbers that could be simulated is in the range, $Re_\lambda \approx 20 \sim 30$. Simulations are performed with a wide spectrum of compressibility levels; here we only report the results obtained by use of two extreme cases: one with a low compressibility level, or pseudo incompressible, and the other with a relatively high level. In the former, the initial value of the normalized density rms is very small, i.e. $\rho_{rms} = \sqrt{< \rho'^2 >}/\rho_0 \approx 0$, whereas in the latter, this value is of order unity. The compressibility level was monitored by adjusting the initial values of the following parameters (Passot and Pouquet, 1987): (1) the rms of the Mach number, $M_t = \sqrt{< M'^2 >}$, and (2) the ratio of the compressible energy to that of the total kinetic energy, χ. Below, we limit the discussion to the results obtained for two cases. In what follows, we refer to pseudo incompressible simulations in which the following values are used initially: $M_t = 0.2$, $\chi = 0.01$, and to compressible simulations in which at the initial time $M_t = 0.6$, $\chi = 0.2$.

The compressibility effects can be manifested by both flow visualization and by considering the global behavior in an integral sense. In the former, the contour plots of the relevant variables constructed from the DNS results show the qualitative behavior, whereas in the latter, the ensemble averages of the simulated results portray the quantitative response. To demonstrate this, in Figs. 1 and 2 we present the contour plots of the density for the pseudo incompressible case and for the compressible case, respectively. A prominent difference between the two cases is the formation of steep gradients in the high compressible case which are not observed in the pseudo incompressible simulations. The regions of high gradients are referred to as shocklets, and consistent with the previous simulations of Passot and Pouquet (1987), appear when the initial levels of density and Mach number fluctuations are high. The effects of increased compressibility can be quantitatively demonstrated by examining the temporal variations of the maxima and minima of the divergence of the velocity, the fluctuating Mach number and the ratio of the compressible to the total kinetic energy. These are presented in Figs. 3-6. In Figs. 3 and 4 the temporal variations of the minimum and maximum values of the divergence of the instantaneous velocity ($\nabla \cdot \underline{V}$) are presented for the pseudo incompressible and for the compressible cases, respectively. Note

that in the low compressible flow, the minimum and maximum values are approximately mirror image of each other (with respect to $\nabla \cdot \underline{V} = 0$). In the high compressible case, however, the maximum and minimum divergence curves are asymmetric. The minimum value of divergence occurs at the normalized time of $t \approx 0.7$. This time corresponds to the onset of formation of the shocklets, and indicates severe compression within the flow. It must be mentioned that the capture of these shocklets by means of global numerical methods (without any artificial dissipation) is rather difficult. With 256×256 collocation points, this was the strongest shock that we were able to capture, and a lower resolution would result in a significant oscillation in the magnitude of the velocity divergence after the appearance of the shock. One must be careful not to confuse these numerical oscillations with compression and expansion waves.

The effects of compressibility are further quantified in Figs. 5-6. For the pseudo incompressible flow, Fig. 5, the magnitude of M_t decreases monotonically, whereas in the compressible case, Fig. 6, the decrease in M_t is interrupted by plateaux. The locations of these plateaux coincide with those corresponding to a rise in the compressible kinetic energy and the local minima of the velocity divergence. Therefore, these locations correspond to the times at which shocklets can be formed in the flow. In the pseudo incompressible flow, the magnitude of χ remains fairly constant, indicating that the initial low level of compressibility remains low at all times.

With the development of the flow, the species field would consequently evolve. To visualize the flow, the contour plots of species A are presented in Fig. 7. Parts (a) and (b) of this figure correspond to the zero and the infinitely fast reaction rate cases, respectively. This figure exhibits the effects of random motion on the distortion of the scalar field and the mixing of the two initially segregated reactants (the contours form parallel lines at $t = 0$). The effects of chemical reaction are to increase the steepness of the scalar gradients and to reduce the instantaneous values of the reactants, as indicated by a comparison between parts (a) and (b) of the figure. The quantitative behavior of the scalar development is depicted in a statistical sense by means of examining the evolution of the PDF's of the conserved Shvab-Zeldovich variable $\mathcal{J}$. This variable is normalized and defined within the region $[0, 1]$. Correspondingly, its PDF, $\mathcal{P}_1(\mathcal{J})$ is always bounded in this region. The temporal variation of $\mathcal{P}_1(\mathcal{J})$ is presented in Fig. 8. It is shown in this figure that at the initial time, the PDF is approximately composed of two delta functions at $\mathcal{J} = 0, 1$,

indicating the two initially segregated reactants A and B. At later times, it evolves through an inverse-like diffusion in the composition space. The heights of the delta functions decrease and the PDF is redistributed at other $\mathcal{J}$ values in the range $[0, 1]$. At even later times, the PDF becomes concentrated around the mean value. Proceeding further in time results in a sharper peak at this mean concentration, and the PDF can be approximated by a Gaussian distribution. This Gaussian type behavior has been observed in previous simulations of Givi and McMurtry (1988), and Eswaran and Pope (1988), and also has been corroborated in a number of experimental investigations.

An interesting character of these PDF's is that throughout their evolution, the simulated results compare remarkably well with that of a Beta density. This is also shown in Fig. 8 by a comparison between the Beta density and the DNS generated PDF's. The Beta density is parameterized with the same first two moments as those of the DNS. Therefore, in all the figures, the results are presented with respect to a time scale (t^*) proportional to the decay of the variance of the scalar $\mathcal{J}$. Higher order moments of the DNS data for the variable $\mathcal{J}$ also show good agreements in comparison with those predicted by the Beta density. This is demonstrated in Figs. 9 and 10, where the normalized kurtosis (μ_4) and superskewness (μ_6) are presented of the random variable $\mathcal{J}$ and the reactant A, respectively. At time zero, these moments are close to unity and monotonically increase as mixing proceeds. For the Shvab-Zeldovich variable $\mathcal{J}$, the magnitudes of the kurtosis and superskewness resulting from the Beta density asymptotically approach the limiting values of 3 and 15, respectively. These correspond to the normalized fourth and sixth moments of a Gaussian distribution as the variance of $\mathcal{J}$ tends to zero (as $t^* \rightarrow \infty$). The DNS generated results are very close to those of the Beta distribution throughout the simulations. However, the limiting value for variance of $\mathcal{J}$ approaching zero can not be obtained in the simulations due to obvious numerical difficulties. In the reacting case, the moments of the scalar A are consistently higher than those of the conserved scalar, but portray similar trends in both Beta density and DNS generated results.

The trends shown above are also observed in the compressible simulations. The profiles of the PDF's and those of the higher order moments and their comparisons with the corresponding parameterized Beta density are presented in Figs. 11-13. Again, the comparison is remarkably good. The main difference between these results and those of pseudo incompressible simulations is the time scale of the decay of the variance by which the PDF is

evolved.† This time scale can not be incorporated into the PDF description in the format employed here. The single-point nature of these PDF's do not allow for any information about the length scales (or any other scales requiring two-point statistics) of turbulence. For a systematic inclusion of the length scale into the PDF and quantitative description of the differences between the results in the two cases, one is required to consider the evolution of the PDF's at two points (at least). Employing the results of DNS to evaluate (or to generate) models for more than one-point-level closures (O'Brien, 1985; Eswaran and O'Brien, 1989) has proven to be a challenging task, and is the subject of current research (Jiang and Givi, 1991).

The results of these simulations indicate that the approximation of a Gaussian PDF for the final stages of mixing of a conserved scalar is well justified. This corroborates the results of laboratory experiments (e.g. Miyawaki *et al.*, 1974; Tavoularis and Corrsin, 1981) and those of other numerical simulations (e.g. Eswaran and Pope, 1988; Givi and McMurtry, 1988). The numerical experiments performed here, however, are similar to most of the laboratory investigations in that they include the results of only one experimental realization. Future numerical experiments using different initializations and/or with better numerical resolution and including three dimensional effects would be logical extensions of this work.

In addition to the Beta distribution approximations, the DNS results also compare very well with the mapping closure recently introduced by Kraichnan (see Chen *et al.*, 1989 and Kraichnan, 1990). This closure has the property of allowing the relaxation of the PDF of a conserved scalar property to an asymptotic Gaussian distribution. Pope (1990b) has utilized this closure for the prediction of PDF evolution in an isotropic homogeneous turbulent flow with an initial double delta distribution (similar to the condition imposed here). He showed that in the context of a one point PDF, the results obtained by this closure compare favorably with the DNS results. However, again there is no length scale information built into the model, and only the evolution of the PDF without any information regarding the time scale of evolution can be predicted. Madnia and Givi (1991) have extended this model for predicting the decay rate of a reacting scalar in homogeneous turbulence. The generated results obtained by applying this model for the prediction of the

† This is not illustrated in the figures clearly, since the time is scaled by the rate of variance decay.

decay rate of a reacting scalar for the cases considered in DNS are shown in Figs. 14 and 15. In these figures, the DNS generated results and those predicted by a Beta density are also shown. The two PDF's (by the mapping closure, and the Beta density) are constructed in such a way to yield the same first two normalized moments of the Shvab-Zeldovich variable as those of DNS. In this context, the predicted results of the decay by both models show good agreements. The agreement for the mapping closure model is rather surprising, considering that this closure was developed for an isotropic, fully three-dimensional turbulent flow. This is probably due to matching of the normalized first two moments. A better test of the model would be its utilization at two-point level, and its comparison with DNS generated results. Also, the agreement between the mapping closure results and those of DNS worsens as the compressibility level is increased. This again is understandable in that Kraichnan's model was developed for a purely incompressible flow without including any compressibility effects.

With the construction of the DNS database, the results are used to construct the PDF's of the scalar quantities within the subgrid. Since the major riddle in PDF modeling is associated with the closure of the diffusion term and not the chemical reaction term, we limit the analysis to that of the generated PDF's of the conserved Shvab-Zeldovich variable. The construction of the PDF's is implemented by placing a coarse (n^2) mesh over the physical space occupied by the fine mesh (N^2). This mesh can be considered as the one to be potentially used in LES. In this way, it is assumed that the LES predicts the averaged results at the centers of the n^2 mesh, and the fluctuations within the coarse grids are to be modelled by an appropriate PDF closure. The actual LES in this case would correspond effectively to simulations with a homogeneous box filter in which the values of the filtered means are constant. This is somewhat analogous to the procedure followed by Schumann (1989). The main difference is the mechanism by which the fluctuations are to be considered. Schumann (1989) simply neglected such effects, but with consideration of the PDF, it may be possible to account for such effects, albeit statistically. Within each cell of the coarse mesh, we have the values of the scalar quantities at $N_\phi = (N/n)^2$ equally spaced points. This means that there is an ensemble of N_ϕ sample points at each location to construct the PDF's. This construction is implemented by statistical sampling of N_ϕ number of data points. The domain of the scalar property $\phi \in [\phi_{min}, \phi_{max}]$ is divided into a number of bins of size $\Delta\phi$, and the number of scalar variables within each of these bins are counted. The PDF of the variable ϕ, denoted by $\mathcal{P}(\xi)$ is calculated in the interval

$\xi \leq \phi \leq \xi + d\xi,\ d\xi \equiv d\phi$, from the definition of the probability:

$$\mathcal{P}(\xi)d\xi = \text{Probability } (\xi \leq \phi \leq \xi + d\xi) \tag{2'}$$

which translates into:

$$\begin{aligned} \mathcal{P}(\xi)d\xi &\equiv \text{Probability Density} \\ &= \frac{\text{Number of elements in the interval } \xi \leq \phi \leq \xi + d\xi}{N_\phi} \end{aligned} \tag{12}$$

The value of N_ϕ is a measure of the width of the filter, in that it determines the scale at which the fluctuations of the scalar field are not accounted for deterministically, but are included in a probabilistic manner by the PDF's. Consequently, the shapes of these distributions are dependent on the magnitude of the sample size N_ϕ. If this value is too small, then there will be a large scatter in the data. If it is too large, then the PDF's correspond to those appropriate for Reynolds averaging and not LES. In this primeval implementation, we have not yet performed an actual LES (using a PDF subgrid closure). Rather, we have focused only on constructing the shapes of the PDF's from the DNS results. These PDF's can again be quantified by the magnitudes of their moments to provide a reasonable *a priori* assessment of the closure for future actual LES.

With the 256^2 available total data, there is a limit on the magnitude of the ensemble data for an *a priori* assessment. Our experience indicated that an ensemble of about 32^2 was the lowest acceptable limit for a meaningful statistical analysis. Therefore, the domain was broken into 8×8 squares, within each the PDF's were constructed. There was also some analysis with 4×4 squares for better statistics. However, since this is very close to the Reynolds averaging limit, the generated results will not be considered in the forthcoming discussions.

The PDF's constructed from this ensemble showed that as the mixing proceeds, all the PDF's tend to have an asymptotic Gaussian distribution. This is to be expected, since a subset constructed from a large random set with a probability distribution tends to portray the same statistical behavior. However, the results showed that for all the cases considered, the PDF's tend to have an evolution similar to that of the Beta density. This is demonstrated in a sample plot of the distributions in Fig. 16 for both pseudo incompressible

and compressible simulations. In this figure, the PDF's within one of the coarse grids are compared with that of a Beta density with the same two first moments as those within the subgrid. The comparison is fairly good, considering the size of sampled data. The overall deviation from the Beta density and the Gaussian distribution in all the subgrids can be quantified by measuring the norms of the deviation of higher moments. The L_2 norms of the fourth moments for the pseudo incompressible and the compressible simulations are shown in Figs. 17 and 18, respectively. Note that at the initial time, the deviation from a Beta distribution is very small and increases with progress in time, but not substantially. At final times, the DNS data are closer to that of a Gaussian distribution, but the magnitudes of the second moments are not small enough for the Beta density to approach a Gaussian distribution. Similar overall trends are also observed for the compressible simulations.

With the results of the analysis, albeit primitive, it is speculated that the approach based on PDF parameterization from its first two moments may prove serviceable for LES, at least for a conserved scalar. However, the approach requires the accurate input of the first two moments of the subgrid which must be provided by modelled LES transport equations. In the absence of a better alternative, the Beta density may prove useful, and the generated results can be used to estimate the maximum reaction conversion rate in the infinitely fast chemistry limit. However, the generalization to include finite rate kinetics may not be very straightforward, since the first two moments (including the covariance of the scalar fluctuations) must be known (or modelled) *a priori*. By the same token, the extension to more complex kinetics with the inclusion of non-equilibrium effects, which are very important for practical applications, remains to be a challenging task.

An improvement of the procedure obviously involves the solution of a transport equation for the PDF (rather than its parameterization with its moments). However, the computational burden may be prohibitive due to the increased dimensionality of the subgrid PDF transport equations. An estimate of the computational requirements indicates that the cost associated with the implementation of LES procedure involving the stochastic solution of the PDF transport equation may be of the same order as that of DNS on the fine grids, unless the ratio of the fine to coarse grid is large. In this regard, the tradeoff between LES and DNS depends on other factors, such as the physical complexity and computational resources.

5. CONCLUDING REMARKS

A spectral collocation algorithm has been employed to study the mechanism of mixing and reaction in a non-premixed, decaying two-dimensional homogeneous turbulent flow. The evolution of the species field in a one-step stoichiometric reaction of the type $A + B \rightarrow Products$ was the subject of the investigation. Calculations were performed for zero-rate and infinitely fast rate chemistry in both pseudo incompressible and relatively high compressible flows. The effects of compressibility are delineated by the formation of thin shocklets and can be quantified by a global examination of the data. Mixing and the reaction conversion rate (in the reacting case) are characterized by examining the evolution of a Shvab-Zeldovich conserved scalar quantity extracted from the DNS. The results show that the PDF of this scalar variable evolves from an initial double-delta function distribution to an asymptotic shape which can be approximated by a Gaussian distribution. During this evolution, a Beta density qualitatively describes the DNS generated PDF's in both pseudo incompressible and compressible simulations. This is quantitatively demonstrated by a good agreement between the values of the higher order moments of the PDF's calculated from the DNS data and those predicted by the Beta approximation. The generated results also compare very well with those predicted with the mapping closure of Kraichnan. The decay of the mean of the reacting scalar determined by DNS compares very well with that predicted by this model and that obtained via the use of the Beta density. This trend is observed in both pseudo incompressible and compressible simulations. The main difference is the time scale of the decay of the variance of the PDF's.

The Beta density seems to also predict the behavior of the fluctuating field within the subgrid for a conserved scalar quantity. Therefore, it may provide a reasonable means of parameterizing the subgrid fluctuations in a stochastic sense. The procedure, however, requires the input of the first two moments of the variable within the subgrid, and these must be provided by modelled LES transport equations. Also, the generalization to include finite rate kinetics may not be very straightforward, since these moments must be modelled *a priori*. An improvement of the procedure involving the solution of a transport equation for the PDF is possible, but may not be practical due to the increased dimensionality of the modelled subgrid PDF transport equations. From the computational point of view, it is recommended to assess the applicability of such a procedure in (yet) simpler flows, before its implementation in simulating more complex flows.

In comparing the DNS results with those of predictions, the first two moments of the Shvab-Zeldovich variable must be matched. This is because single-point PDF's do not include information about the frequency scales of turbulence. Therefore, the evolution of the length scale, or any other parameter requiring two-point information, must be introduced in an *ad hoc* manner (here, such information is provided via DNS). Future validation studies of the PDF's by DNS need to consider the evolution of multi- (at least two-) point statistics. O'Brien (1985) has already employed a two-point formulation in the statistical description of homogeneous turbulent flows. The preliminary results obtained by such formulations are in good agreement with experimental data (Eswaran and O'Brien, 1989). However, a comparison between the predicted results and the DNS data, similar to the ones reported here for single point PDF's is recommended.

Future work should also deal with finite rate chemistry with the inclusion of non equilibrium effects, and also on examining the extension of PDF methods in dealing with the subgrid closures in LES of such flows.

References:

Aldama, A. A. (1990), *Filtering Techniques for Turbulent Flow Simulations*, Lecture Notes in Engineering, vol. 56, Editor: Brebbia, C. A. and Orszag, S. A., Springer-Verlag, New York, NY.

Chen, H., Chen, S. and Kraichnan, R. H. (1989), *Phys. Rev. Lett.*, vol. 62, p. 2657.

Drummond, J. P. (1991), in *Numerical Approaches in Combustion Modeling*, Chap. X, AIAA Prog. in Aeron. and Astr., Editors: Oran, E. S. and Boris, J. P., in press.

Erlebacher, G., Hussaini, M. Y., Speziale, C. G. and Zang, T. A. (1987), *NASA CR 178273*, ICASE Report 87-20, NASA Langley Research Center, Hampton, VA.

Eswaran, V. and O'Brien, E. E. (1989), *Phys. Fluids A*, vol. 1(3), p. 537.

Eswaran, V. and Pope, S. B. (1988), *Phys. Fluids*, vol. 31(3), p. 506.

Ferziger, J. H. (1977), *AIAA Journal*, vol. 15(9), p. 1261.

Ferziger, J. H. (1981), Stanford University Report No. TF-16, Department of Mechanical Engineering, Stanford University, Stanford, CA.

Ferziger, J. H. (1982), in *Recent Contributions to Fluid Mechanics*, Editor: Haase, W., Springer-Verlag, New York.

Ferziger, J. H. (1983), in *Computational Methods for Turbulent, Transonic and Viscous Flows*, p. 93, Editor: Essers, J. A., Hemisphere Publishing Co., New York, NY.

Givi, P. (1989), *Prog. Energy Comb. Sci.*, vol. 15, p. 1.

Givi, P. and McMurtry, P. A. (1988), *AIChE Journal*, vol. 34(6), p. 1039.

Hawthorne, W. R., Wedell, D. S. and Hottel, H. C. (1949) , Third Symposium on Combustion, Flames and Explosion Phenomena, The Combustion Institute, Pittsburgh, PA, p. 266.

Hussaini, M. Y., Speziale, C. G. and Zang, T. A., (1990), in *Whither Turbulence? Turbulence at the Crossroads*, Editor: Lumley, J. L., Lecture Notes in Physics, vol. 357, p. 354, Springer-Verlag, New York, NY.

Ievlev, V. M. (1970) *Izv. Akad. Navk. S.S.S.R. Mekh. Zhidk. Gaza*, vol. 5, p. 91.

Ievlev, V. M. (1973) *Dokl Akad. Navk. S.S.S.R.*, vol. 208, p. 1044 (also, *Sov. Phys.-Dokl.*, vol. 18, p. 117 (1973).

Jiang, T.-L. and Givi, P. (1991), work in progress.

Kraichnan, R. H. (1990), *Phys. Rev. Lett.*, vol. 65, p. 575.

Kuo, Y. Y. and O'Brien, E. E. (1981), *Phys. Fluids*, vol. 24, p. 194.

Libby, P. A. and Williams, F. A. (1980), Editors, *Turbulent Reacting Flows*, Topics in Applied Physics, vol. 44, Springer-Verlag, New York, NY.

Madnia, C. K. and Givi, P. (1991), work in progress.

McMurtry, P. A. and Givi, P. (1989), *Comb. Flame.* vol. 77, p. 171.

Miyawaki, O., Tsujikawa, H., and Uraguchi, Y. (1974), *J. Chem. Eng. Japan*, vol. 7, p. 52.

O'Brien, E. E. (1980), in *Turbulent Reacting Flows*, vol. 44, Topics in Applied Physics, Chap. 5, p. 185, Editors: Libby, P. A. and Williams, F. A., Springer-Verlag, New York, NY.

O'Brien, E. E. (1981), *AIAA Journal*, vol. 19, p. 366.

O'Brien, E. E. (1985), in *Frontiers in Fluid Mechanics*, Editors: Davis, S. W. and Lumley, J. L., p. 113, Springer-Verlag, New York, NY.

O'Brien, E. E. (1986), *Physico Chemical Hydrodynamics*, vol. 7(1), p. 1.

Oran, E. S. and Boris, J. P. (1987), *Numerical Simulations of Reactive Flow*, Elsevier Publishing Co., Washington, D. C.

Passot, T. and Pouquet, A. (1987), *J. Fluid Mech.*, vol. 181, p. 441.

Pope, S. B. (1979), *Phil. Trans. Royal Soc. London*, vol. 291 (1384), p. 529.

Pope, S. B. (1985), *Prog. Energy Comb. Sci.*, vol. 11, p. 119.

Pope, S. B. (1990a), Proceedings of Twenty-Fourth Symposium (Int.) on Combustion, The Combustion Institute, Pittsburgh, PA., in press.

Pope, S. B. (1990b), "Mapping Closures for Turbulent Mixing and Reaction," presented at NASA Langley Research Center on the occasion of the sixtieth birthday of John Lumley. Hampton, Virginia, October 1990.

Reynolds, W. C. (1990), in *Whither Turbulence? Turbulence at the Crossroads*, Editor: Lumley, J. L., Lecture Notes in Physics, vol. 357, p. 313, Springer-Verlag, New York, NY.

Riley, J. J., Metcalfe, R. W., and Orszag, S. A. (1986), *Phys. Fluids*, vol. 29(2), p. 406.

Rogallo, R. S. and Moin, P. (1984), *Ann. Rev. Fluid Mech.*, vol. 16, p. 99.

Schumann, U. (1989), *Atmospheric Environment*, vol. 23(8), p. 1713.

Schumann, U. and Friedrich, R. (1986), Editors, *Direct and Large Eddy Simulation of Turbulence*, Proceedings of the EUROMECH Colloquium No. 199, Munchen, FRG, Sep. 30-Oct. 2, 1985.

Schumann, U. and Friedrich, R. (1987), in *Advances in Turbulence*, Editors: Comte-Bellot, G. and Mathieu, J., Springer-Verlag, New York, NY.

Tavoularis, S., and Corrsin, S. (1981), *J. Fluid Mech.*, vol. 104, p. 311.

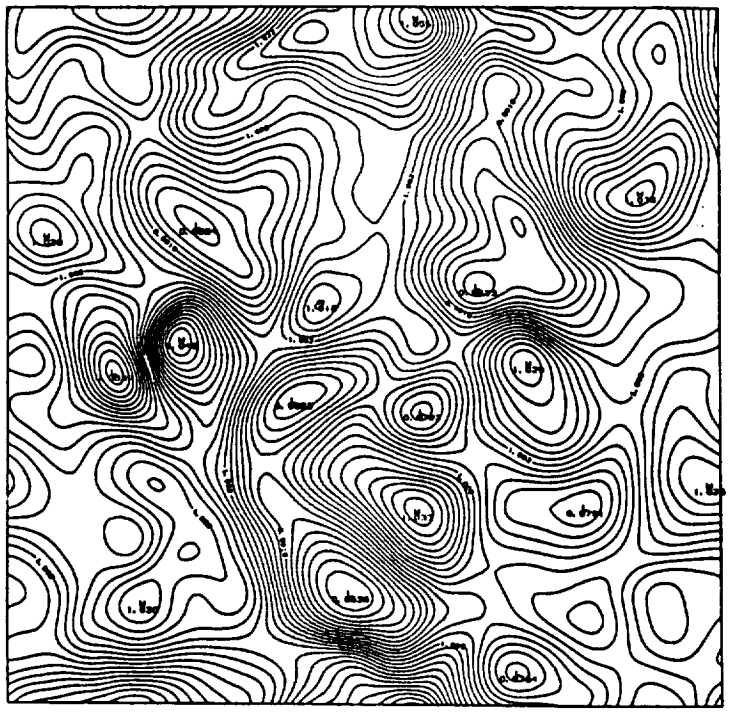

Figure 1. Plot of density contours for the pseudo incompressible case. $t = 6.142$.

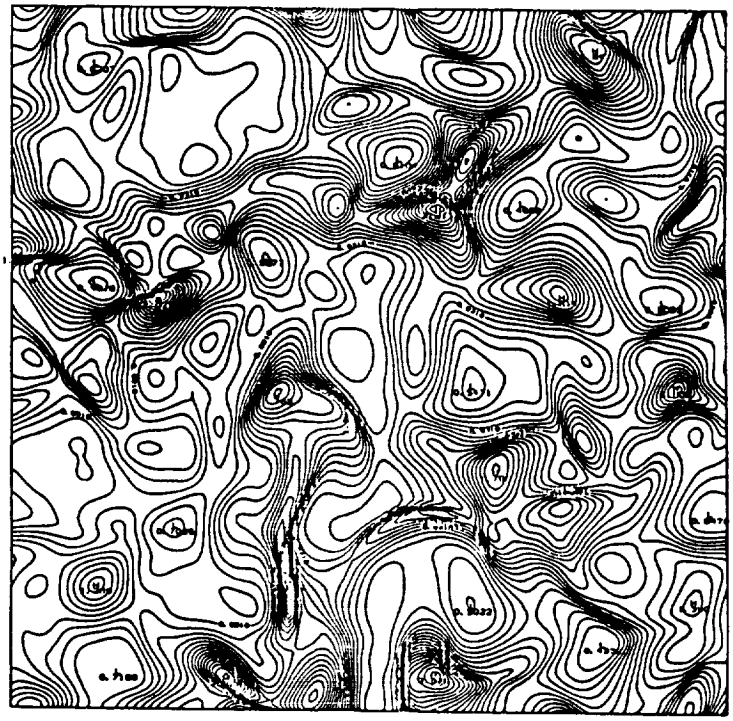

Figure 2. Plot of density contours for the compressible case. $t = 0.686$.

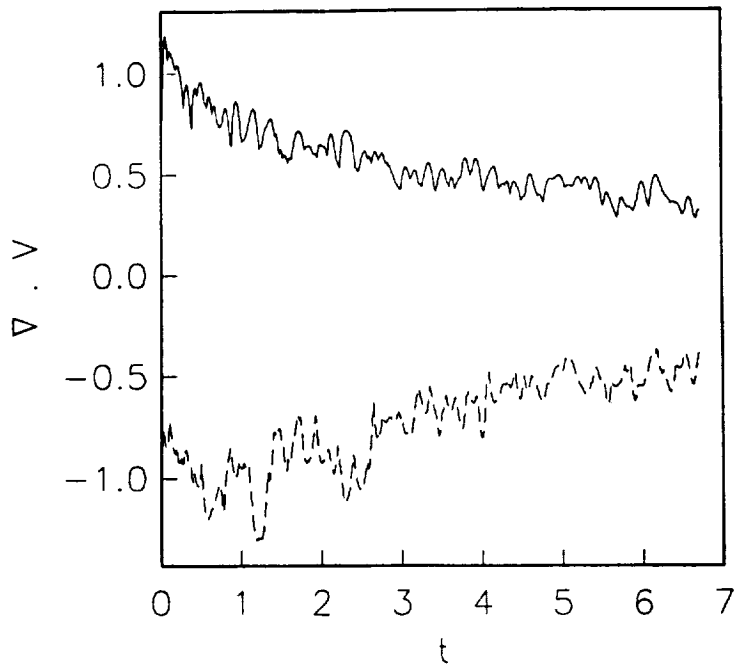

Figure 3. Temporal variation of the minimum and maximum values of velocity divergence for the pseudo incompressible case.

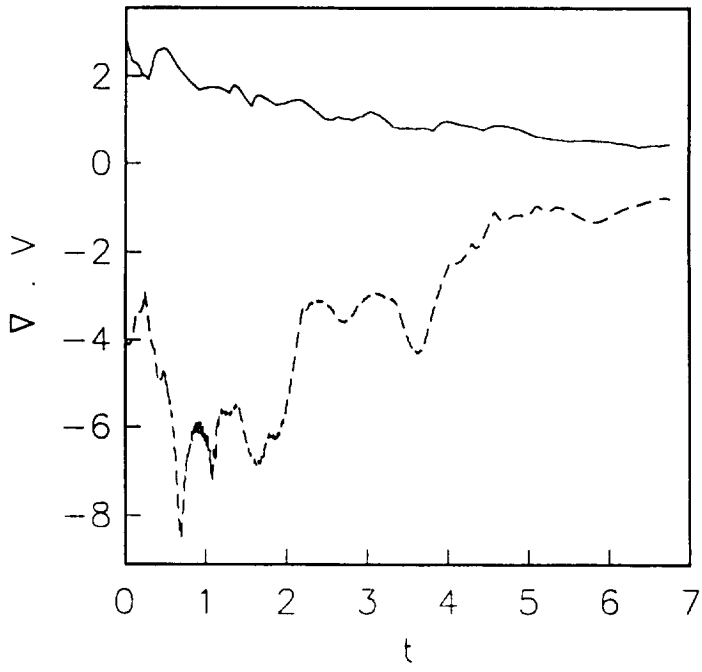

Figure 4. Temporal variation of the minimum and maximum values of the velocity divergence for the compressible case.

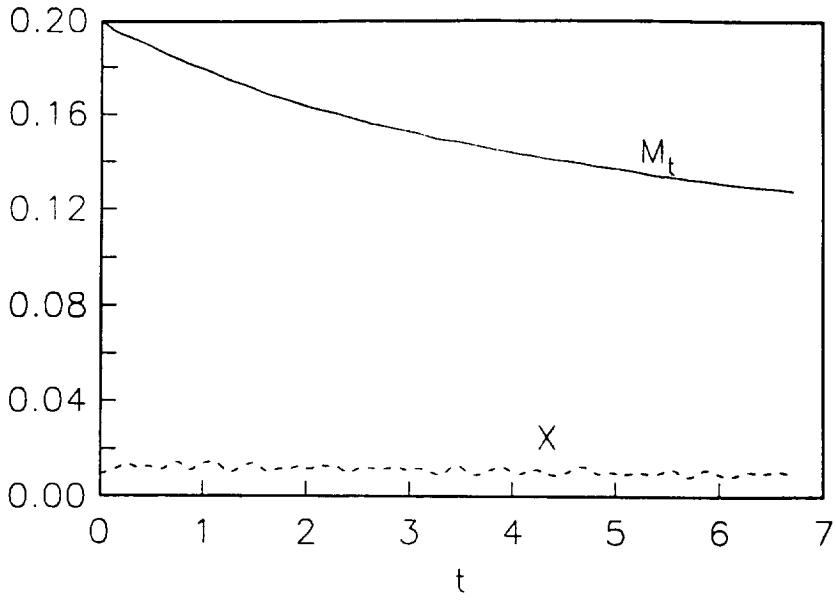

Figure 5. Temporal evolution of M_t (solid line) and χ (dashed line) for the pseudo incompressible case.

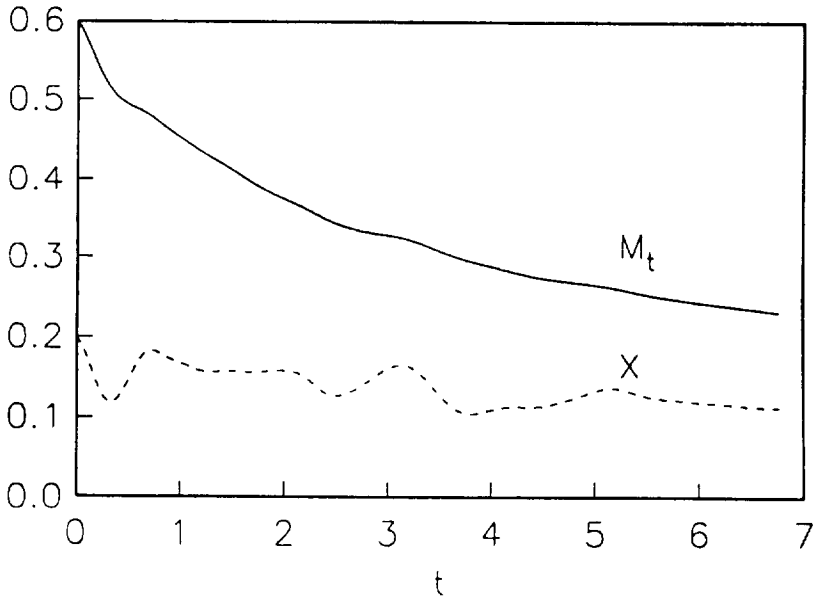

Figure 6. Temporal evolution of M_t (solid line) and χ (dashed line) for the compressible case.

(a)

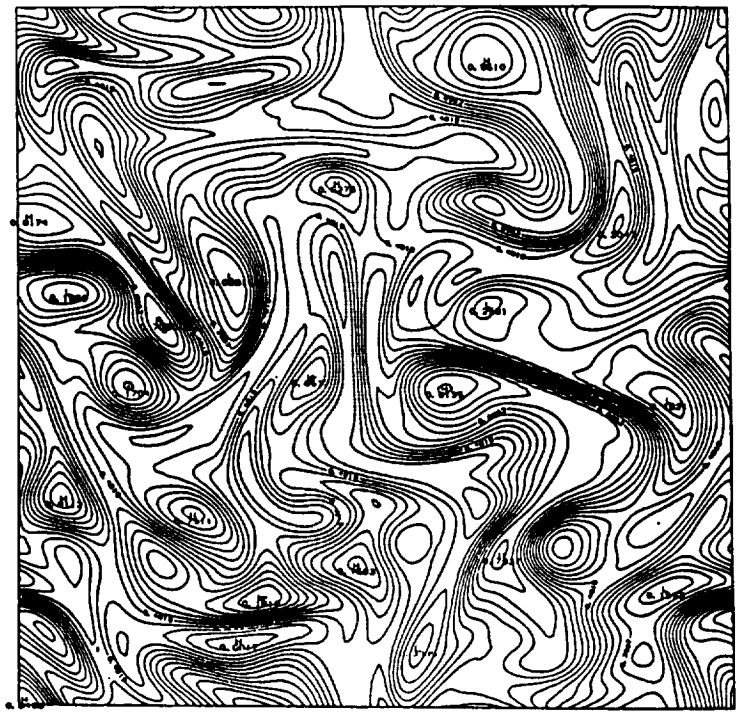

(b)

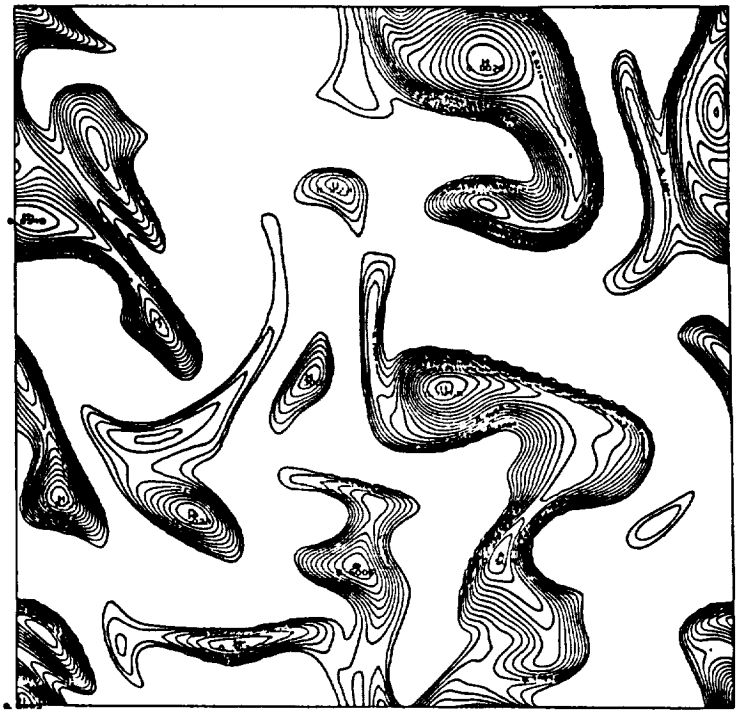

Figure 7. Plot of species A concentration contours at $t^* = 1.0715$. (a) non-reacting case; (b) reacting case.

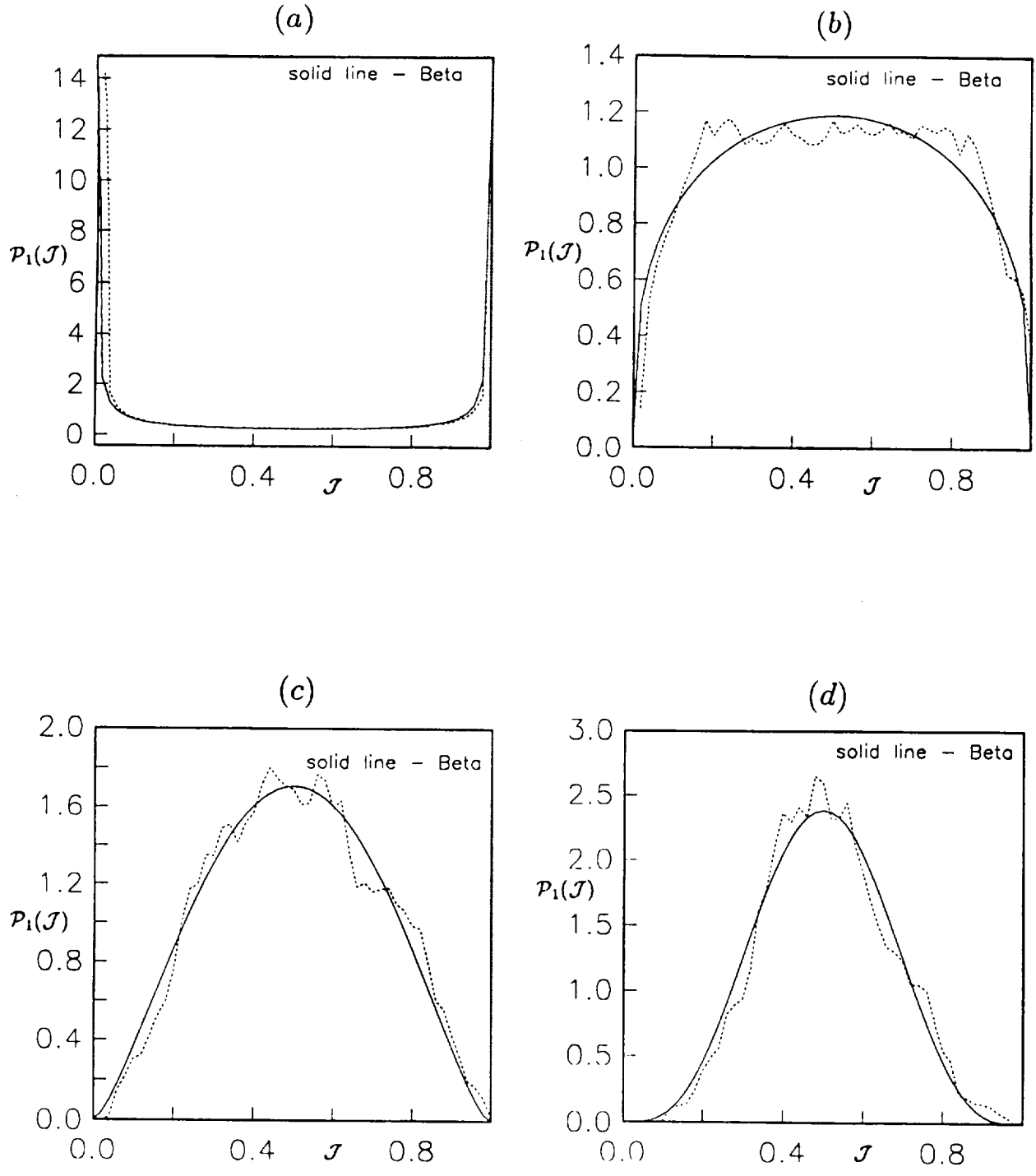

Figure 8. Temporal evolution of $\mathcal{P}_1(\mathcal{J})$ for the pseudo incompressible case. DNS data (dotted line), Beta density (solid line).
(a) $t^* = 0.035$, (b) $t^* = 0.549$, (c) $t^* = 0.800$,
(d) $t^* = 1.0715$.

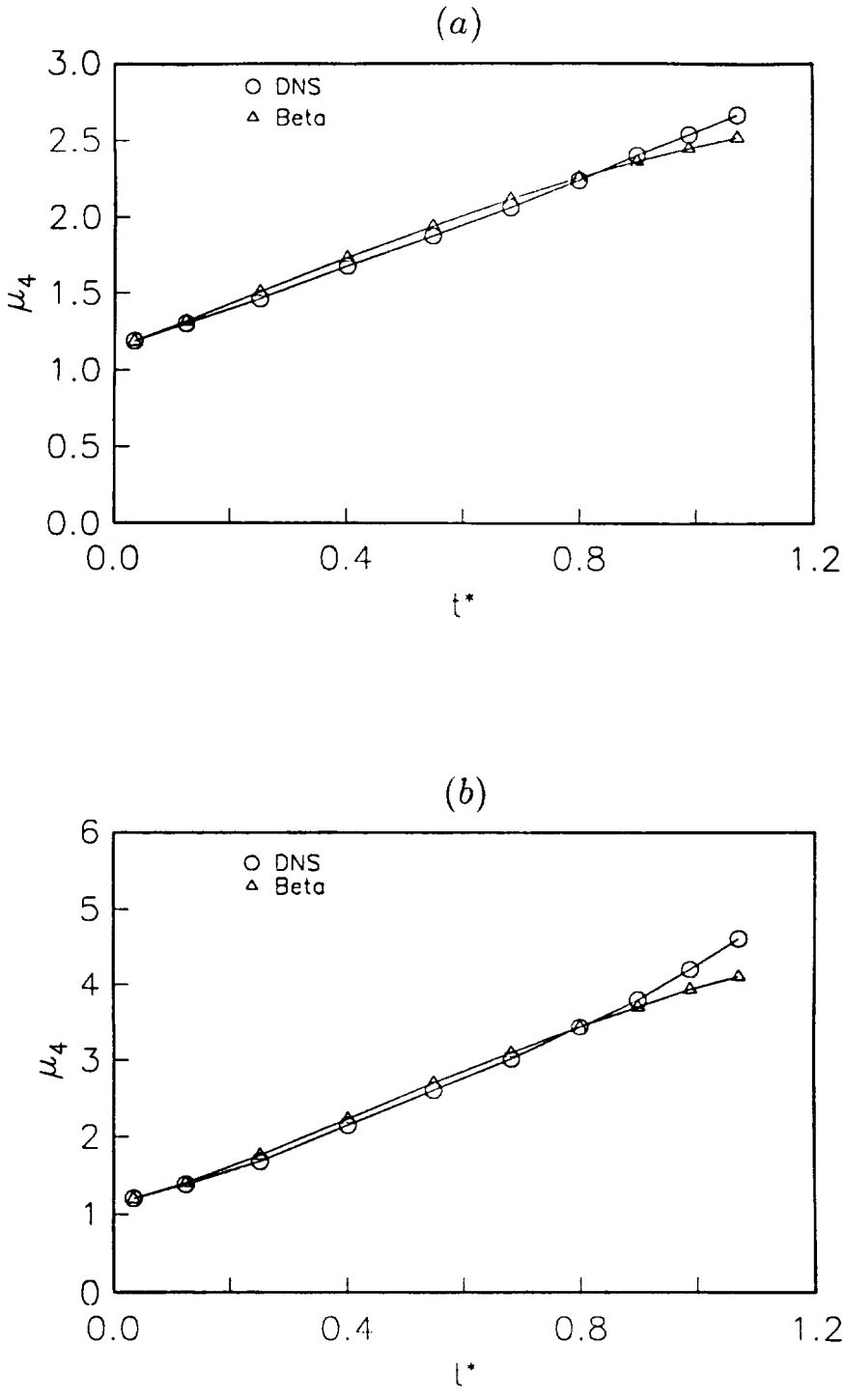

Figure 9. Temporal variation of the kurtosis, μ_4, for the pseudo incompressible case. (a) variable $\mathcal{J}$, (b) Species A in reacting case.

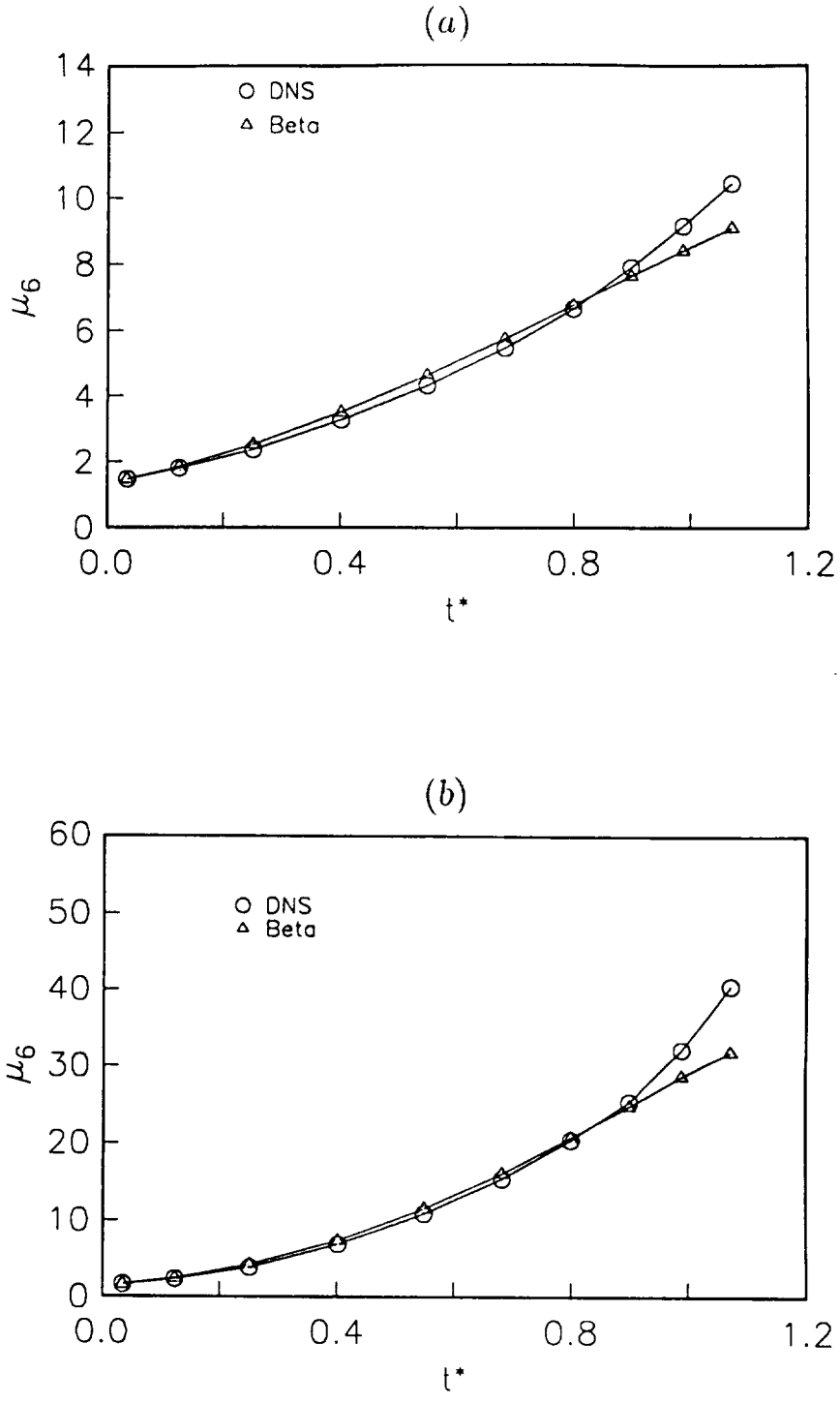

Figure 10. Temporal variation of the superskewness, μ_6, for the pseudo incompressible case. (a) variable $\mathcal{J}$, (b) Species A in reacting case.

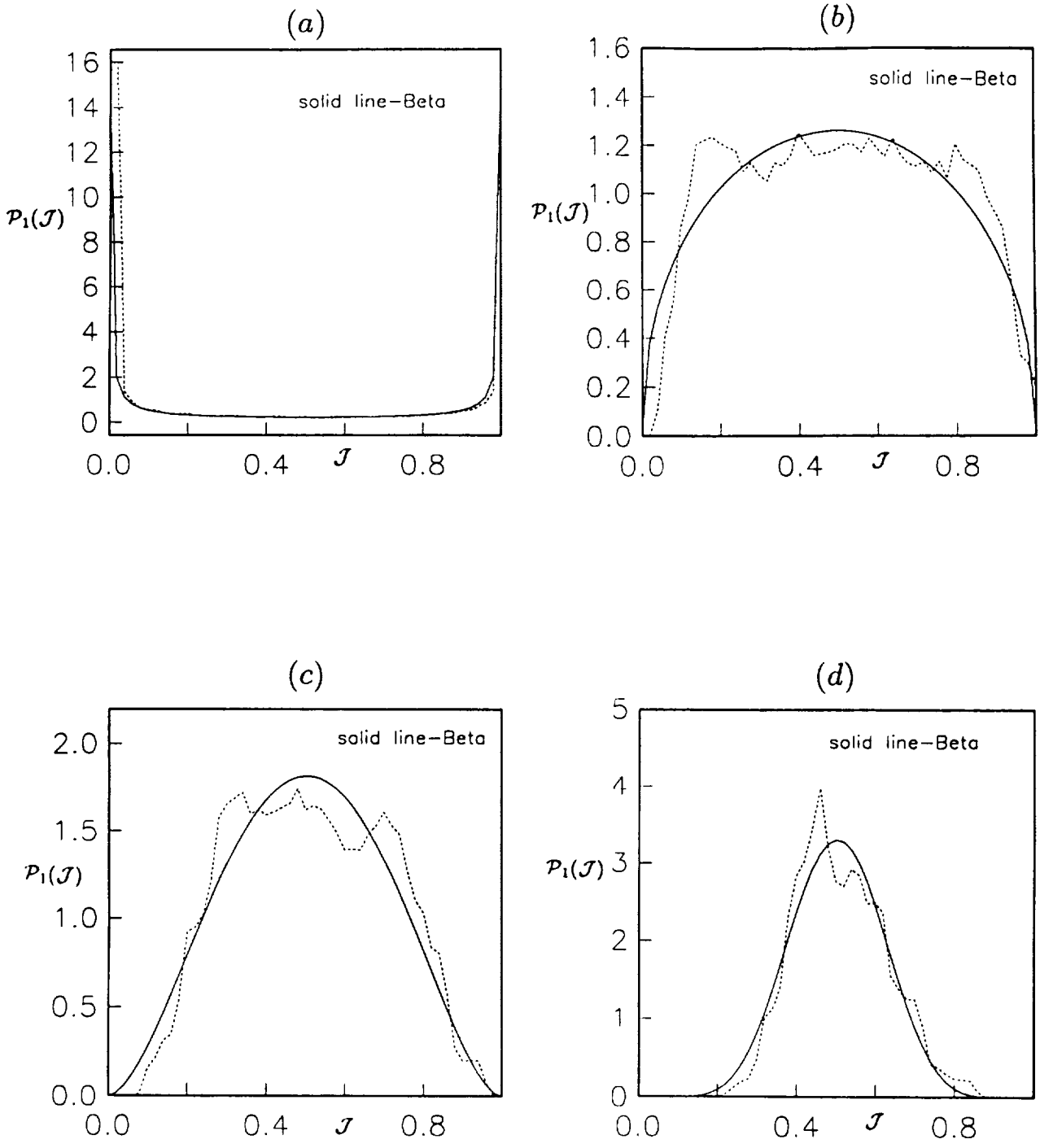

Figure 11. Temporal evolution of $\mathcal{P}_1(\mathcal{J})$ for the compressible case.
DNS data (dotted line), Beta density (solid line).
(a) $t^* = 0.014$, (b) $t^* = 0.587$, (c) $t^* = 0.848$,
(d) $t^* = 1.365$.

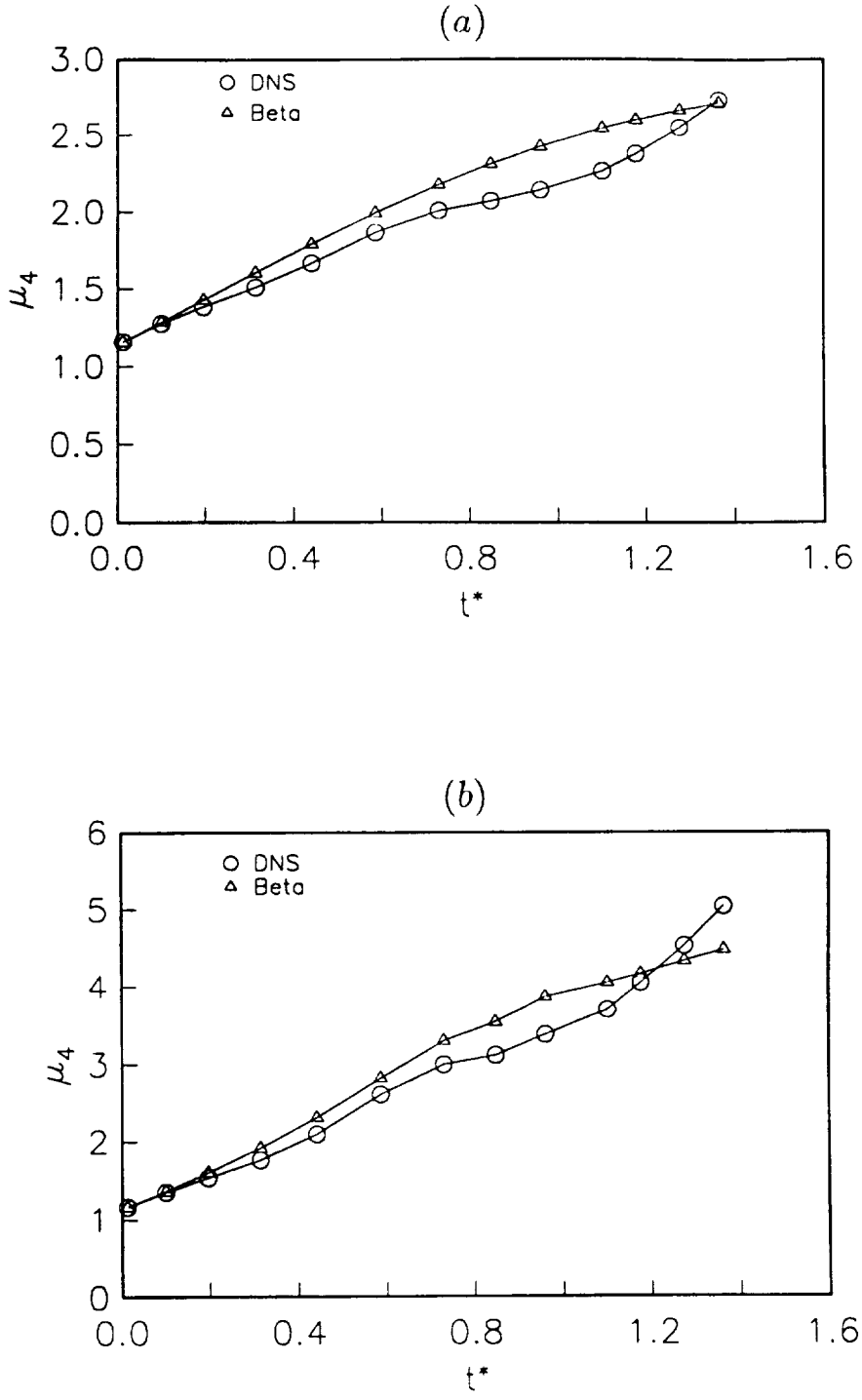

Figure 12. Temporal variation of the kurtosis, μ_4, for the compressible case. (a) variable $\mathcal{J}$, (b) Species A in reacting case.

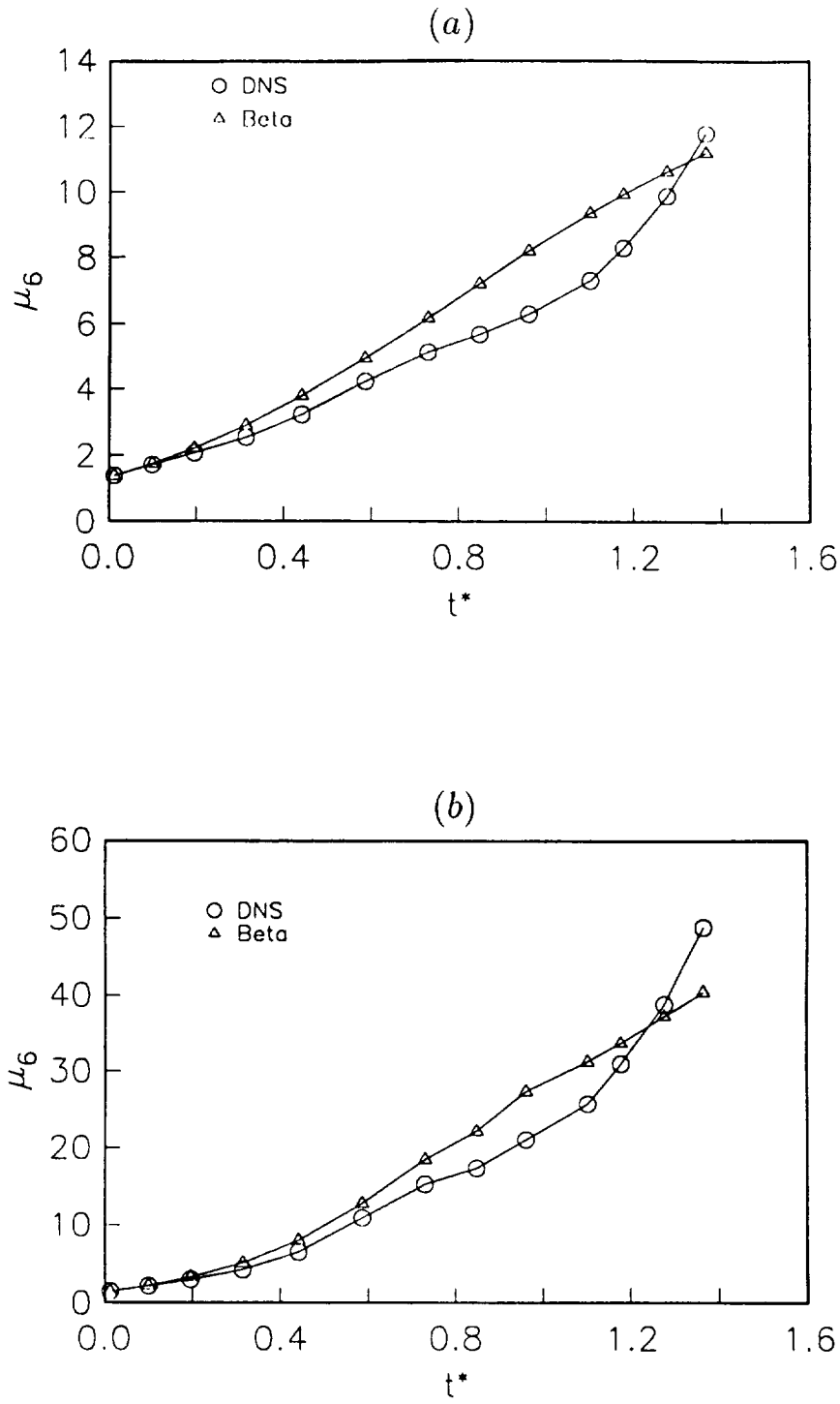

Figure 13. Temporal variation of the superskewness, μ_6, for the compressible case. (a) variable $\mathcal{J}$, (b) Species A in reacting case.

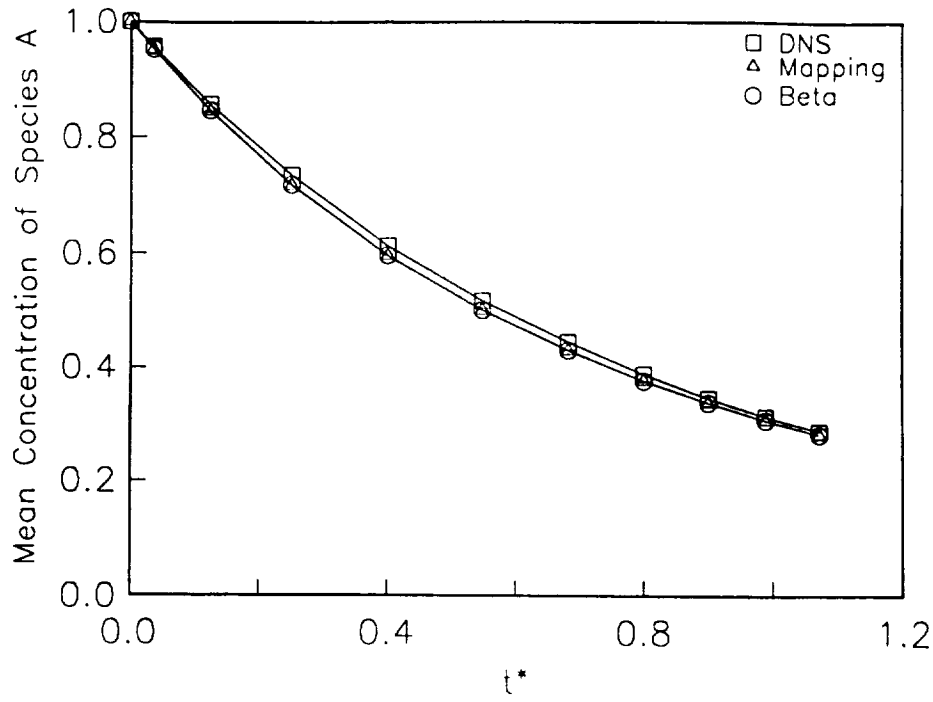

Figure 14. Mean concentration of the reacting species A vs. time for the pseudo incompressible case.

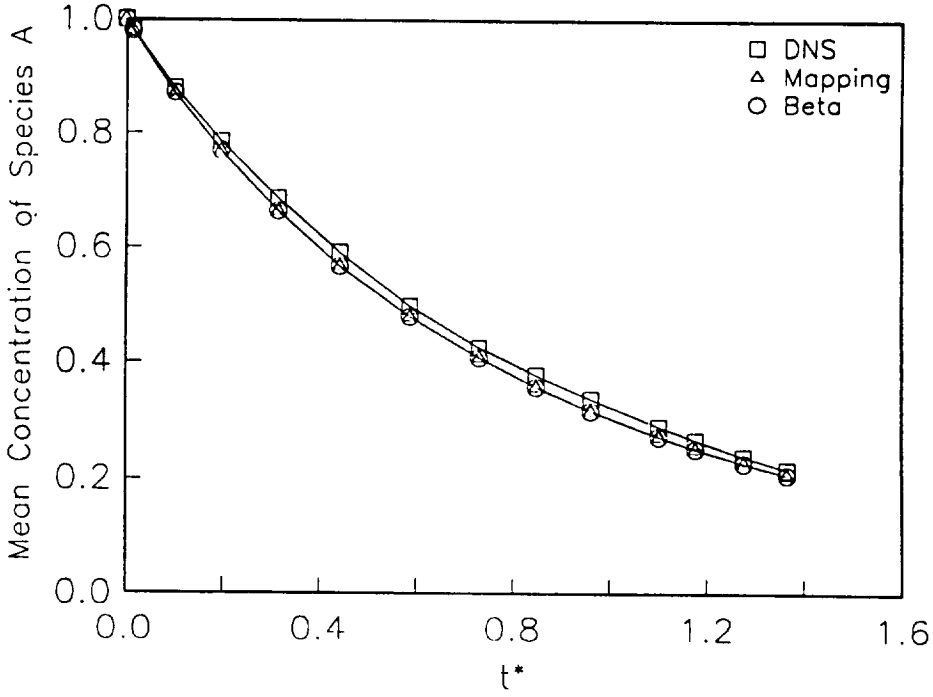

Figure 15. Mean concentration of the reacting species A vs. time for the compressible case.

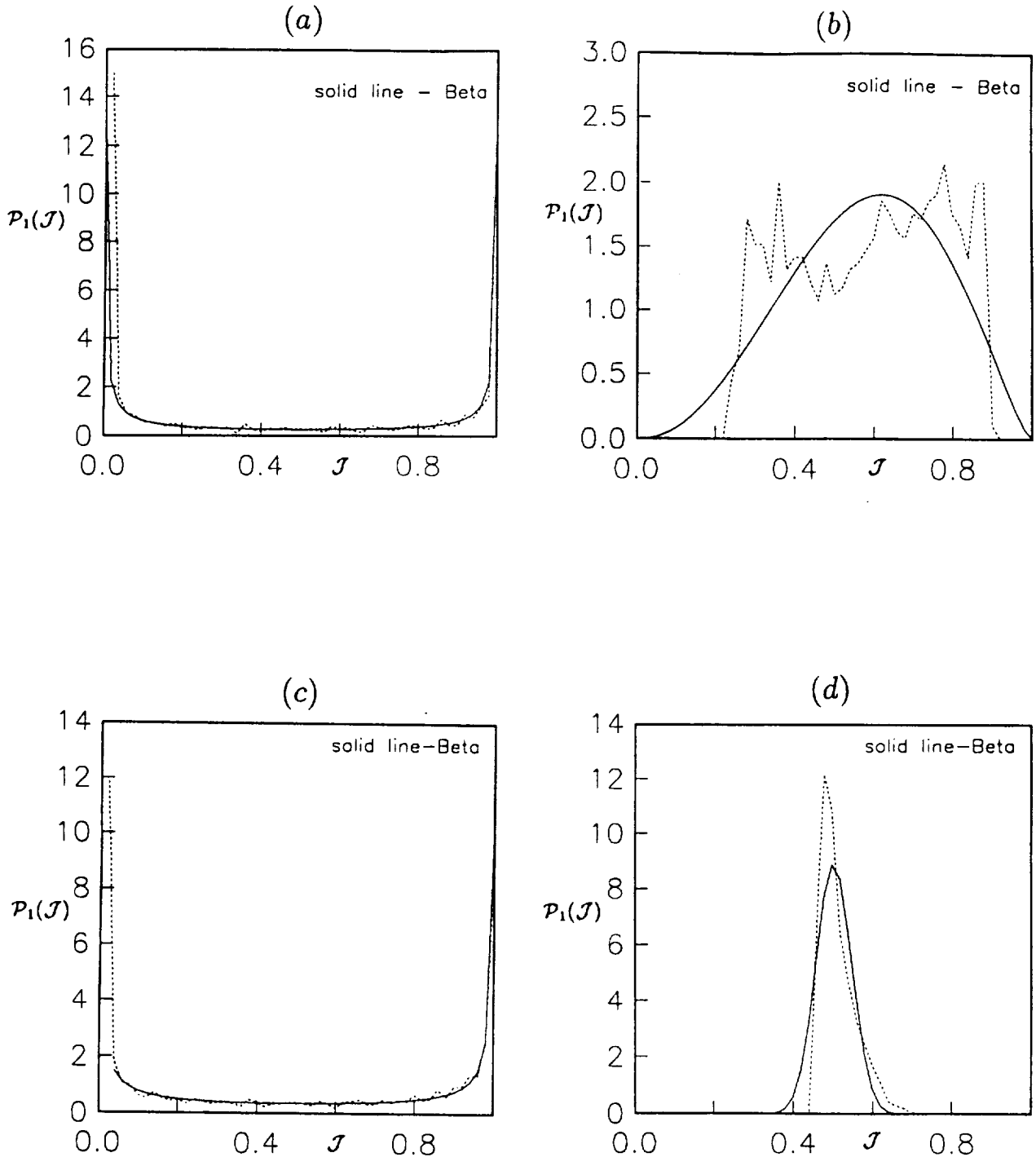

Figure 16. Sample PDF's of the variable $\mathcal{J}$ within the subgrid.
(a) pseudo incompressible case, $t^* = 0.0355$, (b) pseudo incompressible case, $t^* = 0.800$
(c) compressible case, $t^* = 0.101$, (d) compressible case, $t^* = 1.507$.

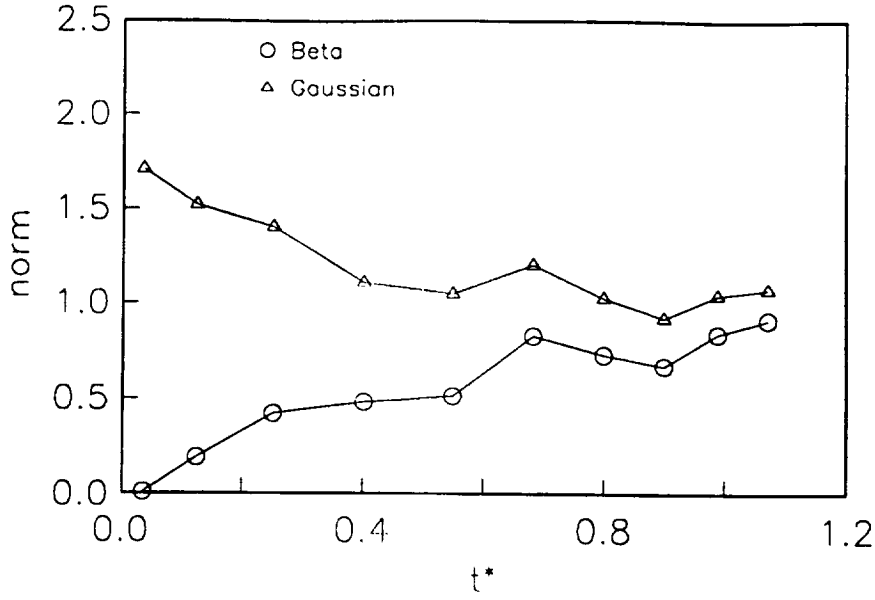

Figure 17. L_2 norm of deviation of the fourth moment vs. time for the pseudo incompressible case.

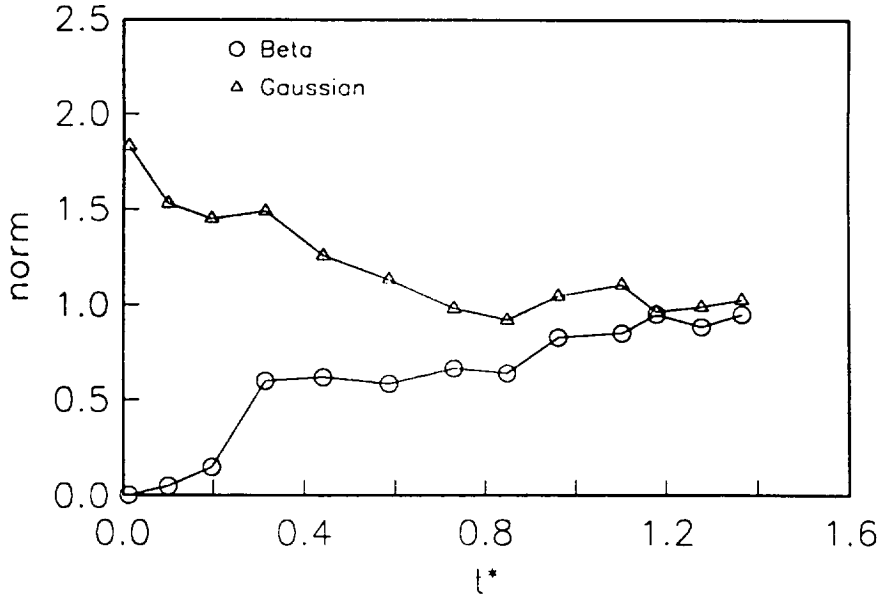

Figure 18. L_2 norm of deviation of the fourth moment vs. time for the compressible case.

Appendix II

The results presented in this Appendix are obtained by Mr. Alex Tsai, who is a M.S. candidate working on this project.

In this Appendix, we demonstrate the capabilities of the EDQNM spectral closure in its implementation in a two-point PDF formulation. In doing so, we present the results obtained by means of the solution of a two-point PDF transport equation in a homogeneous turbulent flow under the influence of a binary reaction of the type $A + B \rightarrow Products$. The turbulent field is statistically stationary, with a specified energy spectrum. The EDQNM model is used for the closure of the convective flux, and the LMSE model is used for the modeling of the molecular mixing. The purpose of this appendix is to show that the EDQNM is indeed capable of predicting the evolution of the length scales, and that the chemistry does not have a significant impact on the evolution of these scales.

In Fig. II.1, we present the temporal evolution of the maximum mean fuel concentration for two different initial values of the integral length scale. This figure shows the exact effects of the length scale. Note that as this scale is smaller, i.e. the reactants are in a closer vicinity of each other, the rate of chemical reaction become larger, and the fuel is consumed faster. This figure displays the "beauty" of two-point formulation! In Fig. II.2, the evolution of the Taylor microscale is presented for the fuel concentration under two limiting conditions of no chemistry and infinitely fast reaction rate. Note that until the final stages of reaction (at long times) the length scales are the same, and the results only deviate slightly at final times. The same is also evident in Fig. II.3, in which the normalized dissipation rates of the scalar quantities are presented. Note that the difference between the two cases is not substantial.

With the results presented above, we conclude that the evolution of the length scales predicted by means of the model described above, is not sensitive to the rate of chemistry. This is validated by considering the scales under the two limiting conditions. However, the model employed for the closure of molecular mixing is based on the LMSE closure. While the results of our preliminary DNS validate the conclusions drawn from these two-point simulations, we would still need to perform more simulations, in order to make this point more clear.

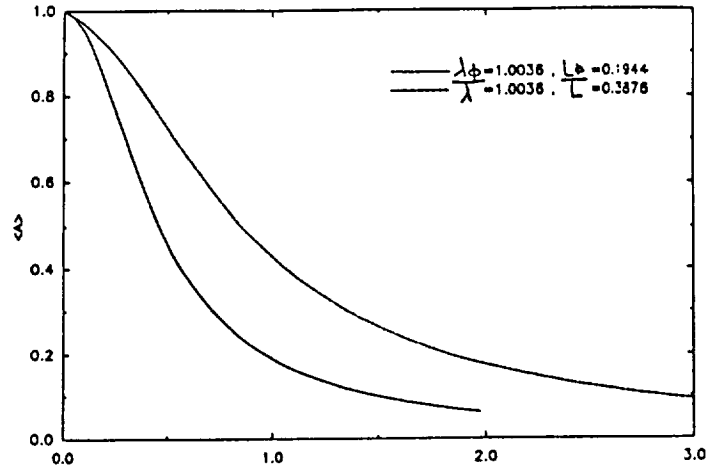

Figure II.1. Temporal variation of $< A >_t / < A >_0$
(Combination of LMSE and EDQNM Closures)

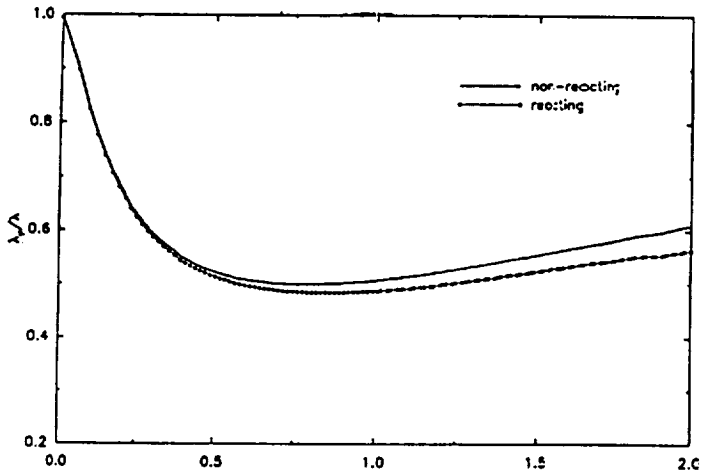

Figure II.2. Temporal variation of the Taylor Microscale
(EDQNM Closures)

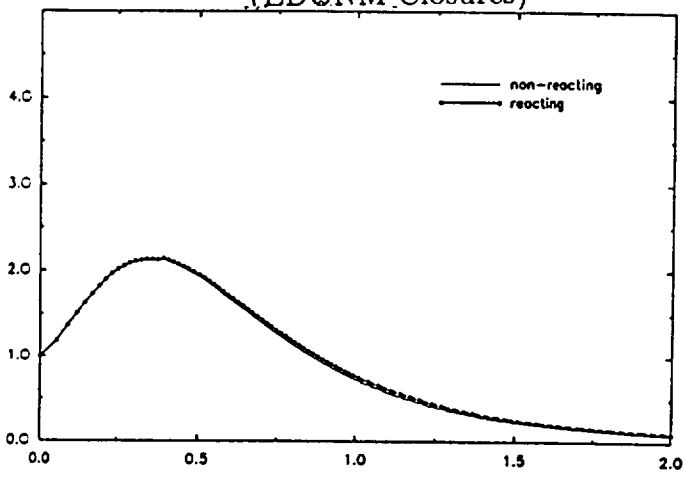

Figure II.3. Temporal variation of the Scalar Dissipation Rate
(EDQNM Closures)

Appendix III

This Appendix is prepared by Mr. Craig Steinberger, a Ph.D. candidate working on this projects.

Model Free Simulations of a High Speed Reacting Mixing Layer

Craig J. Steinberger *
Computational Fluid Dynamics Laboratory
Department of Mechanical and Aerospace Engineering
State University of New York at Buffalo
Buffalo, NY 14260

Abstract

The effects of compressibility, chemical reaction exothermicity and non-equilibrium chemical modeling in a combusting plane mixing layer were investigated by means of two-dimensional model free numerical simulations. It was shown that increased compressibility generally had a stabilizing effect, resulting in reduced mixing and chemical reaction conversion rate. The appearance of "eddy shocklets" in the flow was observed at high convective Mach numbers. Reaction exothermicity was found to enhance mixing at the initial stages of the layer's growth, but had a stabilizing effect at later times. Calculations were performed for a constant rate chemical rate kinetics model and an Arrhenius type kinetics prototype. The Arrhenius model was found to cause a greater temperature increase due to reaction than the constant kinetics model. This had the same stabilizing effect as increasing the exothermicity of the reaction. Localized flame quenching was also observed when the Zeldovich number was relatively large.

1 Introduction

Research on the subject of compressible reacting mixing layers has been of high priority in recent years. Much of this effort has been devoted to the development of high speed air breathing flight vehicles. This type of vehicle would, according to current proposals, use supersonic combustion ramjet (scramjet) engines for propulsion. In such an engine, fuel is injected into a high speed airflow. The mechanisms of mixing and combustion of this non-premixed, high speed, compressible, reacting flow is of great complexity.

The purpose of this study was to investigate the coupling between the hydrodynamic and chemical phenomena that are present in compressible, reacting mixing layers. Although

*Research Assistant, Student Member AIAA.

experimental studies have provided useful results, this avenue of research is often difficult and expensive. Numerical simulation has become widely accepted as an alternative and supplement to experimental investigation. Model free simulations have proven especially useful because there is no need to introduce the potential inaccuracies of a turbulence model. An extensive review of current numerical simulation techniques and results for reacting flows is provided by Givi [1].

1.1 Previous Research

Brown and Roshko [2] found that the turbulent mixing layer is dominated by large scale coherent structures, or vortices. These structures convect at a nearly constant speed and tend to coalesce with neighboring vortices. Papamoschou and Roshko [3] continued these experiments to determine the effect of compressibility on the spreading rate of a supersonic mixing layer. They found that it is useful to study the flow in reference frame that travels with the flow at the same speed as an average large scale structure. A parameter which quantifies the compressibility in the flow was proposed as the convective Mach number, M_c; defined as the Mach number of the flow with respect to the above mentioned frame of reference. A direct correlation was found between M_c and the stability of the flow. Lele [4] replicated the results of [3] by means of direct numerical simulation of a two-dimensional mixing layer. In addition, he noted the appearance of eddy shocklets within the flow for $M_c > 0.7$.

McMurtry, *et al.* [5] studied the effects of an exothermic chemical reaction on the shear layer via direct numerical simulation. In this study, an approximate set of equations that are valid for low Mach number flows was used. It was found that the heat liberated from a chemical reaction causes the layer to grow at a slower rate that of on-heat releasing flow. These results agree with those obtained experimentally. In addition, direct numerical simulations concerned with compressibility and heat release effects on a compressible mixing layer were performed by Givi *et al.* [6].

The phenomenon of flame extinction in non-premixed flames has been the topic of theoretical and experimental study, although direct numerical simulations of such flows have been somewhat limited. Recent reviews of some of the prevalent theories regarding the structure of turbulent non-premixed flames, as well as some of the experimental and numerical work in that field are provided by Bilger [7] and Peters [8].

1.2 Scope of Present Research

The scope of the present work is to examine the effects of compressibility and chemical reaction exothermicity on a reacting plane mixing layer. An examination is also made of the non-equilibrium effects of the chemical kinetics on the structure of a flame. These are accomplished by direct numerical simulation of an unsteady two-dimensional shear layer. The governing equations are integrated via high order finite difference methods, and no turbulence modeling is employed. Since the focus of this study is the general physics of this type of flow, physical modeling is kept as simple as possible so that the above mentioned hydrodynamic and chemical effects may be isolated. The use of simplifying assumptions has the added advantage of saving considerable amounts of computational resources, without reducing the accuracy or validity of the results.

2 Method of Investigation

A two-dimensional version of the SPARK computer code [9, 10] was used to investigate a chemically reacting, compressible, temporally developing mixing layer. The full Navier-Stokes equations as well as the applicable chemical species conservation equations (see [9] or [11] for more detail) were solved via numerical integration. The methods used were the Gottlieb-Turkel finite difference scheme [12] and a dissipative compact parameter method [13]. Both of these algorithms are of fourth order spatial accuracy and second order temporal accuracy.

One of the primary assumptions made in these simulations is that the mixing layer is temporally developing. That is, the reference frame of the simulations is defined to be moving with a velocity equal to that of the mean flow. The advantages of this approximation are twofold. First, with the temporal assumption the inflow and outflow boundary conditions can be assumed to be periodic. The eliminates the problem of specifying downstream boundary conditions. Second, the temporal assumption means that only a relatively small region of the flow is being simulated. This region is then followed in a Lagrangian sense as time progresses. This results in considerable savings in computational resources, which means that the flow may be simulated in greater detail.

The chemical reaction in the flow is assumed to be of a simple, irreversible, second order type of the form

$$A + B \longrightarrow Product + Heat \tag{1}$$

The reaction is characterized by the kinetics mechanism, which is given by the single step

model of

$$\dot{w} = K_f C_A C_B \tag{2}$$

where C_A and C_B represent the concentrations of the reacting species and are assumed equal at the free streams, i.e. $C_{A_\infty} = C_{B_\infty} = C_\infty$. K_f is the reaction rate constant, and can be normalized to form the definition of the Damkohler number, Da:

$$Da = \frac{K_f C_\infty}{U_\infty / \delta_\omega|_0} \tag{3}$$

In the present study two types of chemistry models were used; constant rate kinetics (i.e. constant K_f) and an Arrhenius type model in which K_f varies with the temperature. This is written as

$$K_f = A_f e^{-\frac{Ze}{T/T_\infty}} \tag{4}$$

where A_f is the pre-exponential factor and Ze is the Zeldovich number, defined as

$$Ze = \frac{E}{RT_\infty} \tag{5}$$

Here E is the activation energy and R is the universal gas constant. T_∞ is the free stream temperature. When the Arrhenius kinetic model is used, the pre-exponential factor A_f replaces K_f in the definition of Da (Eq. 3).

Combustion exothermicity is measured by the energy liberated by the chemical reaction, $\Delta H°$. The magnitude of this energy is parameterized by a non-dimensional heat release parameter Ce, defined by:

$$Ce = \frac{-\Delta H°}{c_v T_\infty} \tag{6}$$

Thus, $Ce = 0$ corresponds to a non-heat releasing chemical reaction.

The flow was initialized with a hyperbolic tangent streamwise velocity profile, with reactant A on the top half of the layer with a free stream velocity of $+U_\infty$ and reactant B on the bottom half with a free stream velocity of $-U_\infty$. This flow configuration is shown schematically in Fig. 1. There was no initial fluid motion in the transverse direction, and the pressure was assumed to be initially constant throughout the flowfield. Depending on the problem simulated, the temperature was either assumed to be initially constant or had an initial Gaussian distribution. In most cases, the mixing layer was perturbed by numerical truncation errors. However, when necessary, harmonic forcing was explicitly added to trigger the flow instabilities. For a majority of the simulations, a 128 × 128 point grid was used, with grid compression in the areas of the flow with the sharpest gradients. In those cases

where the gradients were too strong for the details of the flow to be resolved, a 256 × 256 point grid was used.

All parameters are normalized when appropriate by initial or free stream conditions. Time is normalized by

$$t^* = \frac{t}{l_0/U_\infty} \tag{7}$$

3 Sample Results

3.1 Effects of Compressibility

The effect of compressibility on the mixing layer was investigated by varying M_c, the convective Mach number over a range of values from $M_c = 0.2$ to $M_c = 1.2$. The vorticity thickness vs. normalized time for different values of M_c is given in Fig. 2. This figure clearly shows that the growth rate of the vorticity thickness is decreased with increased compressibility. Compressibility also affects the time needed for the layer to roll up into a vortex, which is shown in the figure as a jump in vorticity thickness. Valuable information may be obtained from examination of the variation in the transverse direction of the normalized average streamwise component of the velocity and the normalized mean square streamwise velocity fluctuations. The average streamwise velocity profile is shown in Fig. 3. The most significant feature of these curves is the steepness of the mean velocity profiles at high convective Mach numbers. This shows a sharper velocity gradient across the layer, implying a lesser rate of mixing. The degradation of mixing has the effect of retarding the progress of the chemical reaction. The suppression of turbulence fluctuations with compressibility is shown by the profiles of the mean square of the fluctuating velocity in Fig. 4. A marked decrease in the amplitude of the fluctuations can be observed.

Another feature of the increased compressibility is the formation of eddy shocklets as a result of increased compression after the formation of large scale structures. These shocklets are formed for both subsonic and supersonic free stream flows in order to adapt to high pressure at the braids. An example of this can be seen upon examination of Mach number contours, shown in Fig. 5. This phenomenon has not been observed in any of the experiments on compressible shear layers, to date. This might be caused by the fact that the simulations are two-dimensional, whereas a laboratory flow is dominated by small scale three dimensional transport. It is anticipated that future three dimensional simulations will clarify the matter.

3.2 Effects of Reaction Exothermicity

Calculations were also performed to assess how reaction exothermicity affects the mixing layer. Results are presented of simulations for constant rate kinetics with heat release values of $C_e = 0$, 1.5, and 6. One set of calculations was performed using Arrhenius type kinetics with $C_e = 1.5$ and $Ze = 10$.

The results of these simulations presented in the form of plots of the voriticity thickness versus normalized time (Fig. 6). This figure shows that the rate of growth is highest for the no-heat release case ($C_e = 0$), and, as the heat release parameter is increased, the growth of the layer slows. The relatively smooth regions of voriticity thickness growth may be attributed to diffusion thickening, and a jump in vorticity thickness represents vortex roll-up. For the $C_e = 0$ case, the layer responds to background perturbations fairly quickly, and vortical structures are formed at $t^* \approx 3$. An increase in the magnitude of the heat release results in a delay of vortex roll-up, and the jump in vorticity thickness does not occur until $t^* \approx 7$. Further increase of the heat release parameter results in additional delays, as can be seen for the case of $C_e = 6$. This behavior is also observed for the Arrhenius model with $C_e = 1.5$. In these two cases, the effects of exothermicity are most pronounced; vorticity roll-up does not occur at all, and the only growth in the thickness of the mixing layer is due to molecular diffusion.

The influence of the heat release on the structure of the flame is demonstrated by examining the product thickness of the layer, defined by the normalized total product concentration of the layer as a function of time (Fig. 7). At initial times, the effect of heat release is an enhanced product formation, while the reverse applies at the intermediate and final stages. Initially, the effect of heat release is to expand the fluid at the cores of the layer. A large mixing zone is formed, which results in an enhanced reaction and an increased product formation. This explains the increased initial product thickness. However, as the heat release increases and the layer thickens, the growth of the instability modes become subdued, postponing the formation of the large scale vortices. After initial times, the non-heat release ($C_e = 0$) and $C_e = 1.5$ cases predict a sharp increase in the product thickness. This is caused by the dynamics of the large scale structure formation. The mechanism of roll-up causes the reactants to be entrained into the layer from their prospective free streams. This produces an increase in the extent of mixing, reaction, and product formation. The lack of roll-up in the $C_e = 6$ and Arrhenius cases means the only mixing process is molecular diffusion. Since in these simulations the diffusion mechanism is not as efficient as the roll-up of vortices in the mixing of reactants, the product thickness is correspondingly lower.

3.3 Flame Extinction

Another area of study was the nonequilibrium effects leading to local flame extinction. Simulations were run for large values of the Zeldovich number for an Arrhenius kinetics model and for a constant rate kinetics chemistry model as a control. To obtain the vortex roll-up necessary to this analysis, explicit harmonic forcing was added to the initial conditions of the flow. A forcing amplitude of 0.5% of the mean velocity was used. The most unstable frequencies were found by a linear stability analysis of an equivalent incompressible flow. It was found that if the flow was excited only by the most unstable frequency, two vortices form but they do not pair. If the first subharmonic is added, the vortices undergo pairing.

In the case of large Zeldovich numbers, it was observed from the simulations that, after roll-up and pairing, the flame undergoes local extinction at the braids. This behavior is depicted in contour plots of the reaction rate at times $t^* = 1$, 1.5, 2.25, and 2.5. These contours are shown in Fig. 8 for time $t^* = 1$, when the vortices have just formed. The reaction rate is highest along the mixing surface of the layer, that is, in the center of the intervortex braids. The contours at time $t^* = 1.5$ (Fig. 9) portray the behavior at the initial stages ofS pairing. The reaction rate has begun to decrease in the braids of the emerged vortex. At time $t^* = 2.25$, shown in Fig. 10, the layer has completed the pairing process and strong gradients are observed in the vortex braids. Since the braids are "stretched" as the vortex rotates, they are the area of the highest strain. The flame at the onset of extinction is shown in Fig. 11. Note that the reaction rate has gone to zero at the braids. Product concentration contours (not shown) indicate that very little product exists in these extinguished regions, demonstrating that the flame did not quench due to depletion of reactants. At this point in time, the flame is not continuous, forming what will be called for lack of a better term, a "flame eddy."

This extinction phenomenon has been explained by Peters [8] as follows: At the regions of high strain, the reactants are supplied at a faster rate than they can be consumed by the flame. Thus the local temperature in that area drops and the flame becomes very rich with reactants. As a result, the flame is quenched in that area. If a fast chemistry model or an equilibrium chemistry model is used, the extinction mechanism can not be captured. Investigation of such phenomena requires finite-rate chemistry simulation such as that presented here.

4 Conclusions

Direct numerical simulations of a compressible, temporally developing, reacting plane mixing layer were performed. Several simplifying assumptions were made so that the effects of the variation of isolated parameters could be studied in detail. In particular, the chemical reaction was assumed to be of the general form, $A + B \rightarrow Products + Heat$, and thermodynamic properties were assumed constant and identical for all species.

Studies of various flow phenomena were performed by varying one representative nondimensionalized parameter while keeping all other parameters constant. The convective Mach number, M_c, was used to describe compressibility, the heat release parameter, C_e, represented the exothermicity of the reaction, and the Damköhler number and the Zeldovich number described the rate of the reaction.

The simulations concerning the effect of compressibility on the mixing layer showed a direct correlation between increased compressibility and increased stability (along with reduced turbulence). When the convective Mach number was increased, the rate of growth of the mixing layer, which was measured by the growth of the vorticity thickness, was markedly reduced. Degradation of the development of the streamwise fluctuating velocity and mean velocity profiles was also noted. For high compressibility cases, "eddy shocklets" were observed within the flow. This has been previously reported in two-dimensional simulations, but has not been observed in experiments or in three-dimensional studies to date. An expansion of this work into three dimensions is suggested for future work in this area.

Increased exothermicity was observed to slow the growth of large scale structures. At the initial stages of development, high heat release increased the amount of product formed via volumetric expansion of the core of the layer. However, the heat release caused the layer to be Aless responsive to perturbations, reducing the growth of the layer at later stages. The overall effect of increased heat release, therefore, was to stabilize the flow and to decrease the extent and efficiency of the reaction.

The selection of chemical kinetics model was shown to have significant effect on the development of the flow. The introduction of an Arrhenius chemistry model had a stabilizing effect, thus degrading the progress of the reaction. Non-equilibrium chemistry effects due to the chemistry model was also studied. It was found that at high Zeldovich numbers, the flame would be quenched at regions with large local values of the strain rate.

Acknowledgements

The guidance and support of Dr. Peyman Givi, director of the Computational Fluid Dynamics Laboratory at the State University of New York at Buffalo, is gratefully appreciated. This work is sponsored by NASA Langley Research Center under Grant NAG 1-1122 and by NASA Lewis Research Center under Grant NAG 3-1011. All simulations were performed on Cray-2 and Cray YMP supercomputers with resources provided by the NAS program at NASA Ames Research Center, the NCSA at the University of Illinois. and NASA Langley Research Center. Thanks are also due to Drs. Phil Drummond and Mark Carpenter at NASA Langley, and to Dr. Cyrus Madnia at SUNY at Buffalo for valuable discussions on the subject.

References

[1] P. Givi, "Model free simulations of turbulent reactive flows," *Prog. Energy Comb. Science*, vol. 15, no. 1, pp. 1–107, 1989.

[2] G. L. Brown and A. Roshko, "On density effects and large structure in turbulent mixing layers," *J. Fluid Mech.*, vol. 64, pp. 775–816, 1974.

[3] D. Papamoschou and A. Roshko, "Observations of supersonic free shear layers," AIAA Paper 86-0162, 24th Aerospace Sciences Meeting, Reno, Nevada, January 1986.

[4] S. K. Lele, "Direct numerical simulation of compressible free shear flows," AIAA Paper 89-0374, 27th Aerospace Sciences Meeting, Reno, Nevada, January 1989.

[5] P. A. McMurtry, J. J. Riley, and R. W. Metcalfe, "Effects of heat release on the large scale structures in a turbulent reacting mixing layer," *J. Fluid Mech.*, vol. 199, pp. 297–332, 1989.

[6] P. Givi, C. K. Madnia, C. J. Steinberger, M. H. Carpenter, and J. P. Drummond, "Effects of compressibility and heat release in a high speed reacting mixing layer," to be published in *Combustion Science and Technology*, 1991.

[7] R. W. Bilger, "Turbulent diffusion flames," *Ann. Rev. Fluid Mech.*, vol. 21, pp. 101–135, 1989.

[8] N. Peters, "Laminar diffusion flamelet models in non-premixed turbulent combustion," *Prog. Energy Comb. Sci.*, vol. 10, pp. 319–339, 1984.

[9] J. P. Drummond, "Two-dimensional numerical simulation of a supersonic, chemically reacting mixing layer," NASA TM 4055, NASA Langely Research Center, 1988.

[10] M. H. Carpenter, "A generalized chemistry version of SPARK," NASA CR 4196, NASA Langley Research Center, 1988.

[11] F. A. Williams, *Combustion Theory*. The Benjamin/Cummings Publishing Company, Menlo Park, CA, 2nd ed., 1985.

[12] D. Gottlieb and E. Turkel, "Dissipative two-four methods for time dependent problems," *Mathematics of Computations*, vol. 30, pp. 703–723, October 1976.

[13] M. H. Carpenter, "A family of dissipative compact two-four schemes." submitted to *Journal of Computational Physics*, 1990.

Figures

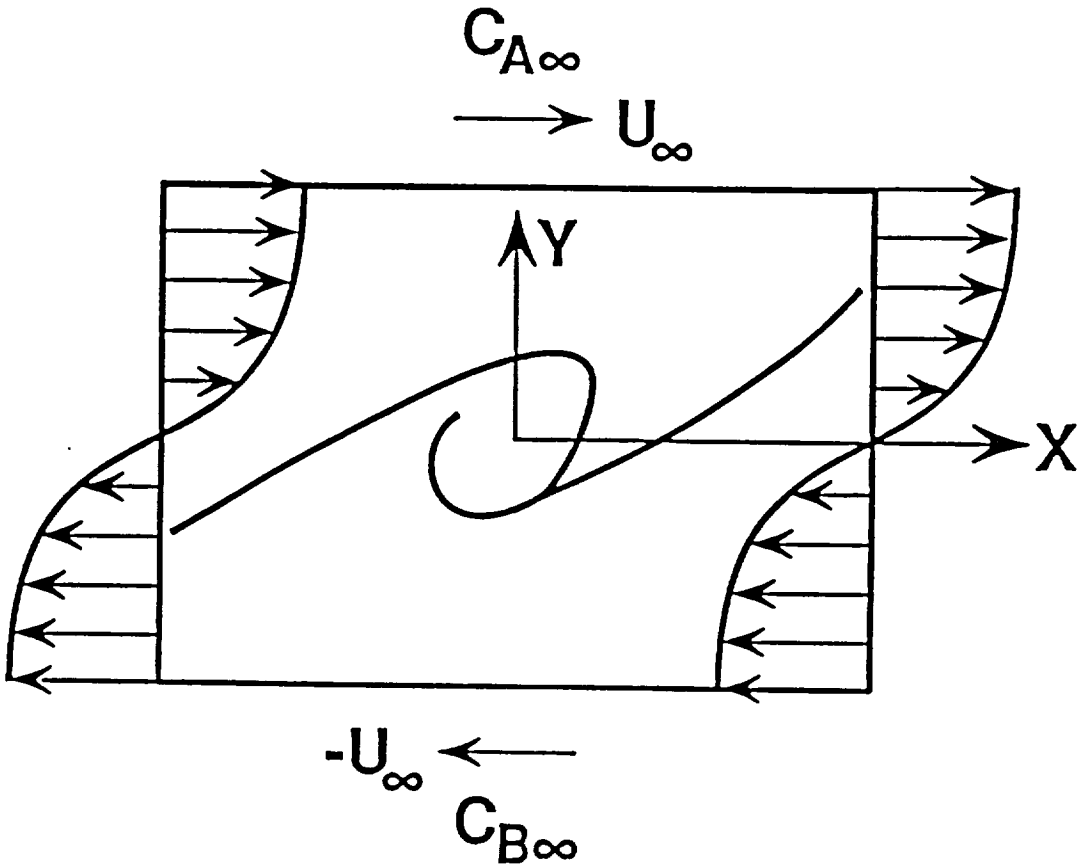

Figure 1: Schematic diagram of a temporally evolving mixing layer.

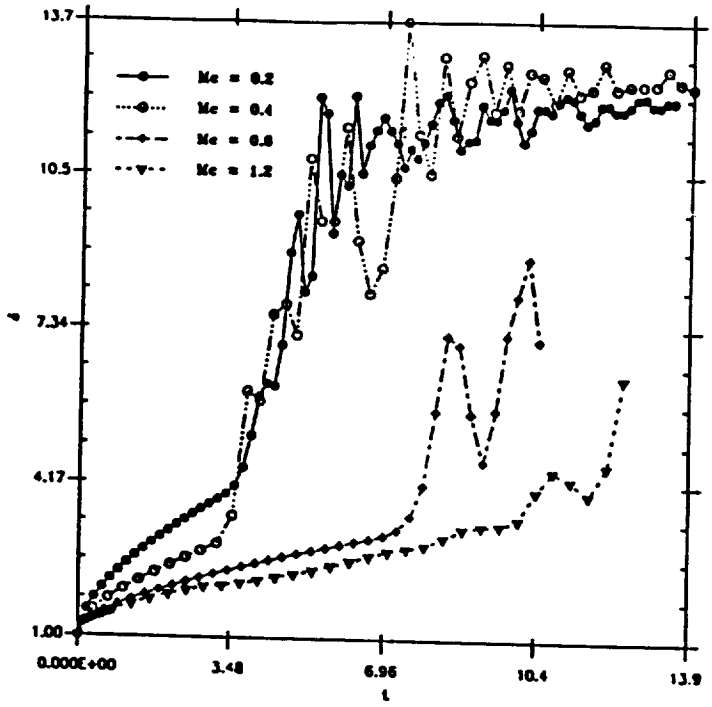

Figure 2: Normalized vorticity thickness versus normalized time for different values of the convective Mach number.

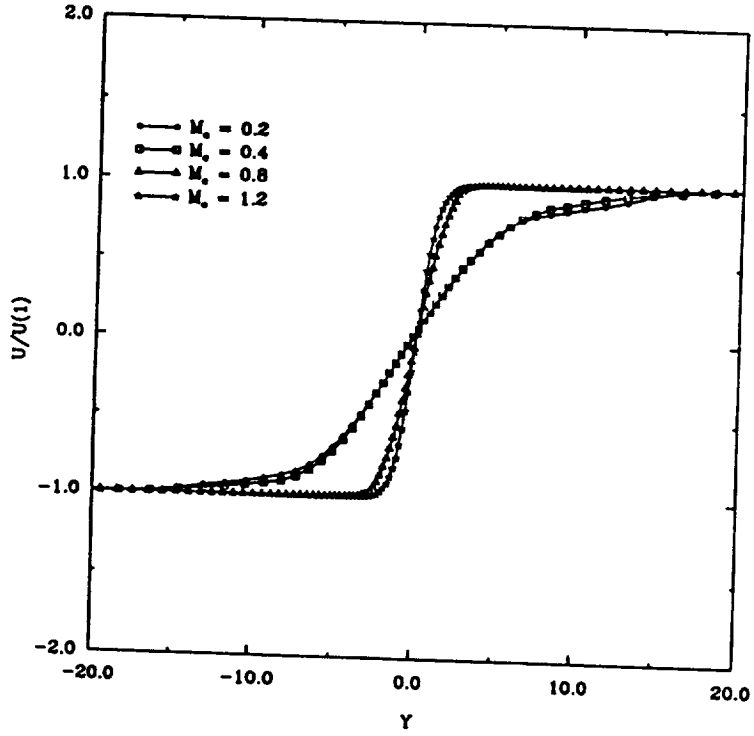

Figure 3: Profiles of normalized mean streamwise velocity for different values of the convective Mach number at time $t^* = 8$.

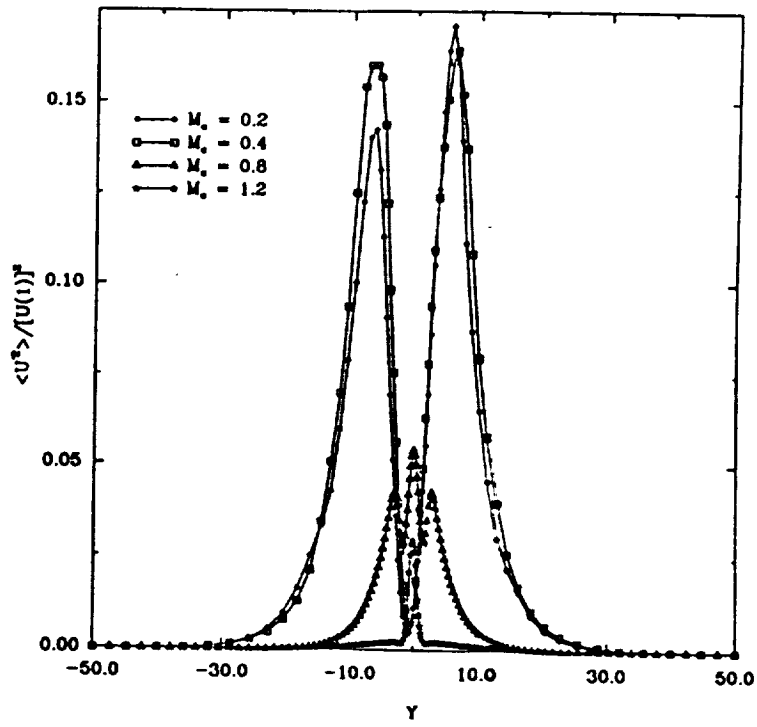

Figure 4: Profiles of normalized mean squared streamwise velocity for different values of the convective Mach number at time $t^* = 8$.

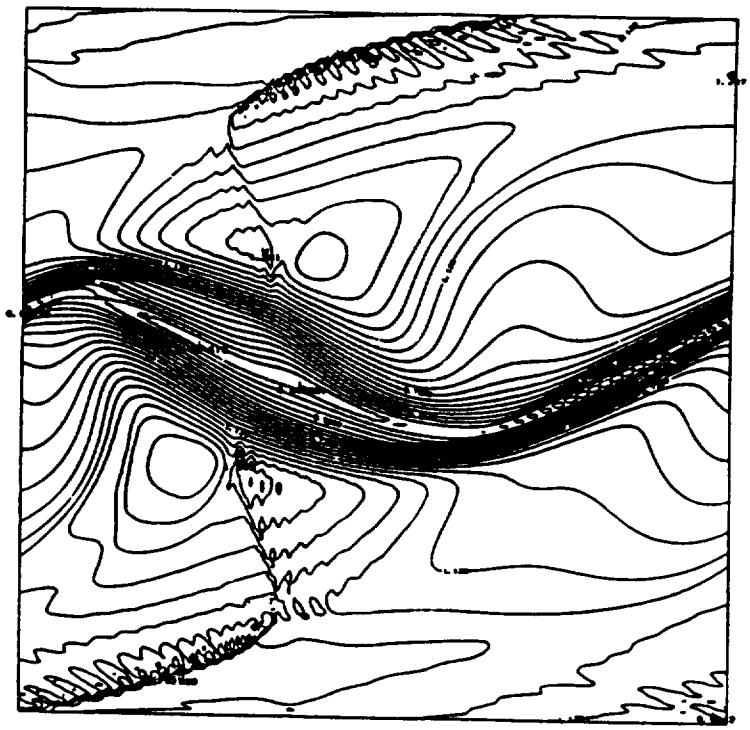

Figure 5: Plot of Mach number contours at time $t^* = 11.66$, $M_c = 1.2$.

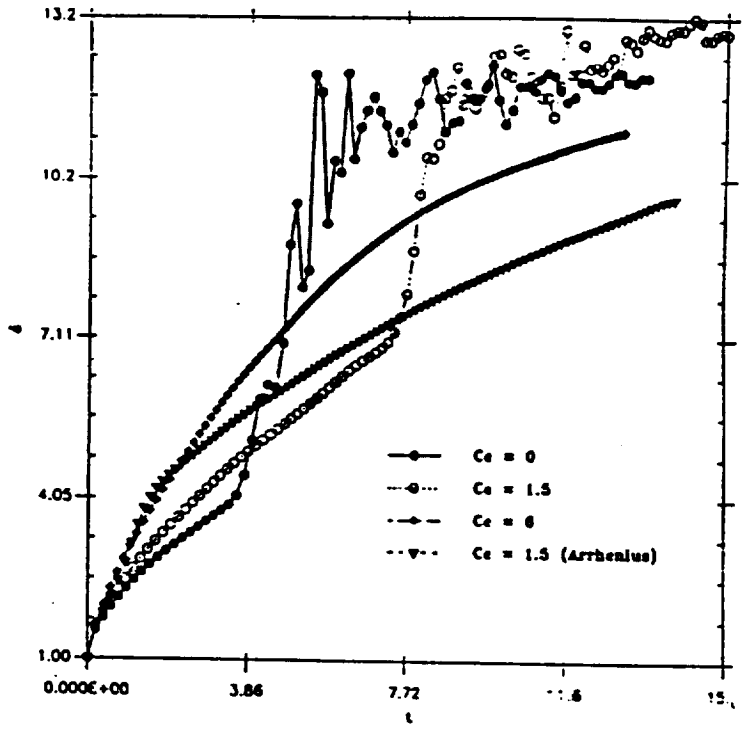

Figure 6: Normalized vorticity thickness versus normalized time for different values of the heat release parameter.

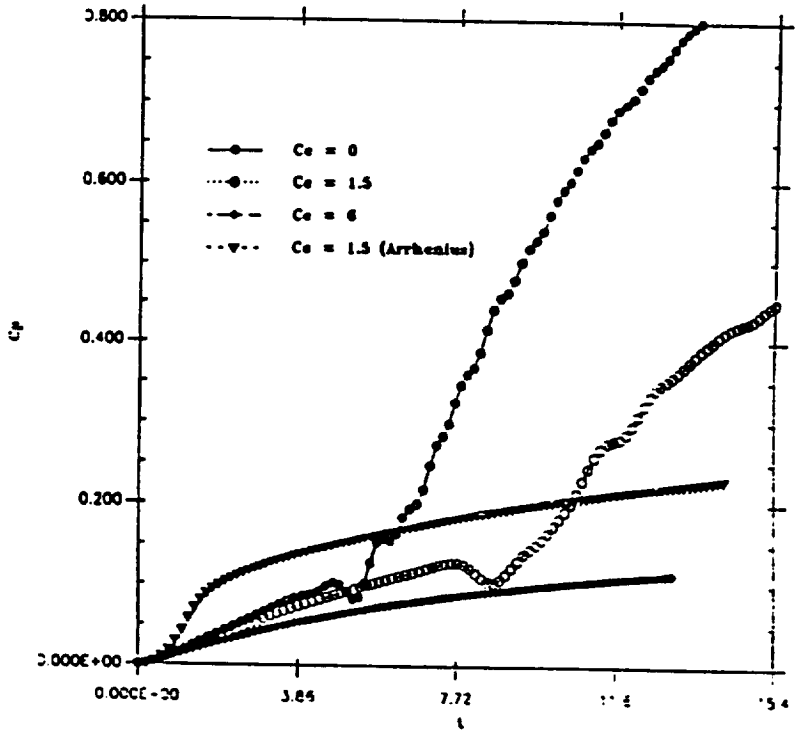

Figure 7: Normalized product thickness versus normalized time for various values of the heat release parameter.

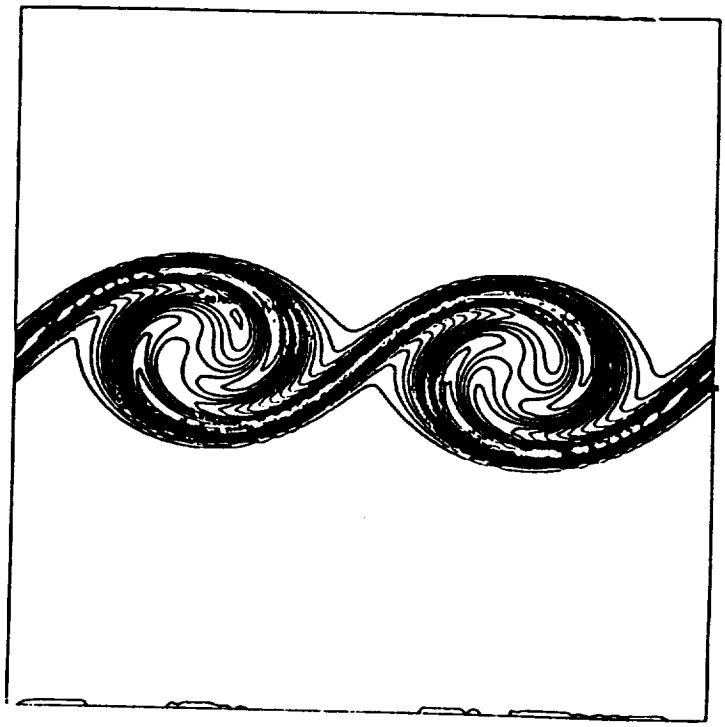

Figure 8: Plot of reaction rate contours, $Ze = 20$, $t^* = 1$.

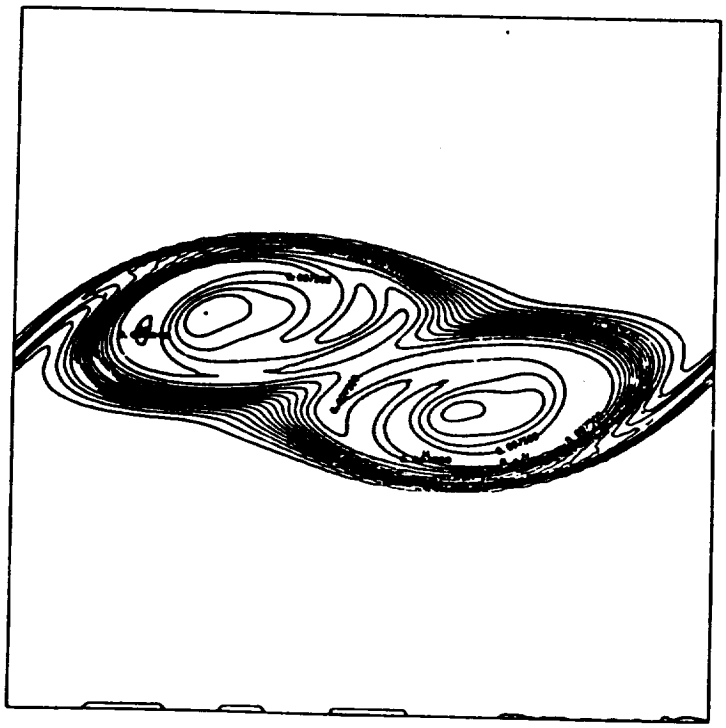

Figure 9: Plot of reaction rate contours, $Ze = 20$, $t^* = 1.5$.

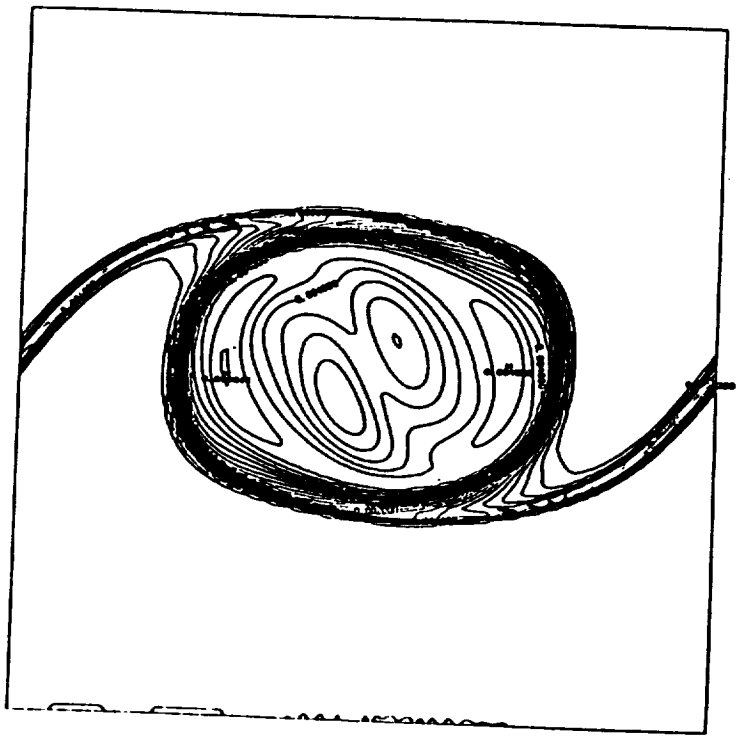

Figure 10: Plot of reaction rate contours, $Ze = 20$, $t^* = 2.25$.

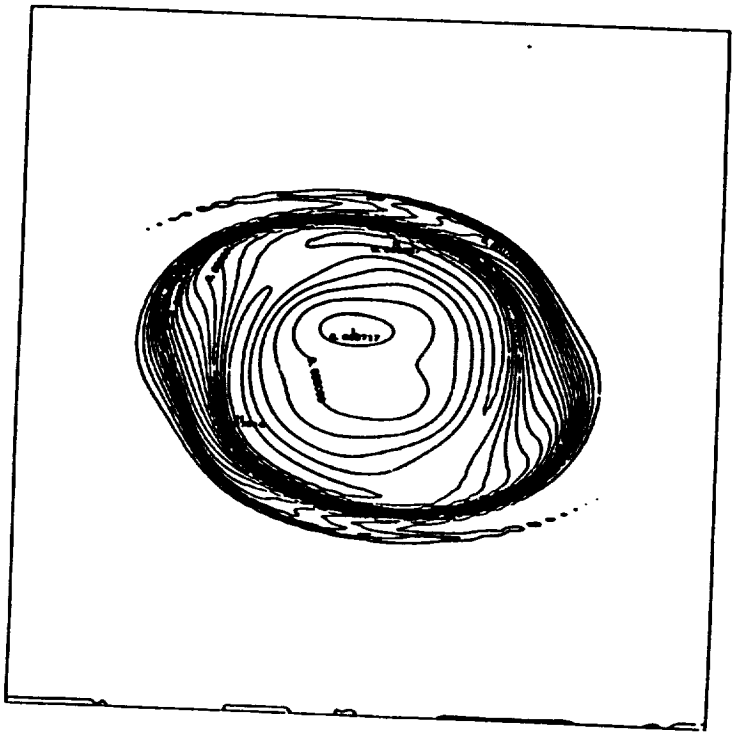

Figure 11: Plot of reaction rate contours, $Ze = 20$, $t^* = 2.5$.